

Bachelor's Degree in Energy Engineering
2016-2017

Bachelor Thesis

PREPARATION AND CHARACTERIZATION OF
EVA/CU NANOPARTICLES NANOCOMPOSITE
MATERIALS FOR POTENTIAL ELECTRICAL
APPLICATIONS

Manuel Meco Gómez

Mentor

Jorge Teno Díaz

Leganés, July 2017



Esta obra se encuentra sujeta a la licencia Creative Commons **Reconocimiento – No Comercial – Sin Obra Derivada**

Index

1. Abstract.....	4
2. Introduction and objectives.....	5
2.1. Objectives.....	6
2.1.1. General approach.....	6
2.1.2. Specific goals.....	6
3. Fundamentals	7
3.1. Polymer composite materials	8
3.1.1. Polymer nanofibers.....	8
3.2. Composites with electrical properties.....	8
3.3. Ethylene-Vinyl Acetate (EVA) Copolymers.....	9
3.4. Cu nanoparticles	12
3.5. Fabrication process	13
3.5.1. Origin and common methods to generate polymeric nanofibers	13
3.5.2. How Solution Blow Spinning works?.....	14
3.5.3. Theoretical approach to Solution Blow Spinning process	15
4. Experimental part	17
4.1. Materials	18
4.1.1. Commercial EVA.....	18
4.1.2. Solvents.....	20
4.1.3. Cu nanoparticles	22
4.2. Fabrication process	23
4.2.1. Elements of the SBS equipment.....	23
4.2.2. How to perform an experiment?	25
4.2.3. Optimization phase	26
4.3. Sample preparation	27
4.3.1. Solution preparation	27
4.3.2. Films preparation. Working conditions.....	32
4.3.3. Films preparation. Experiment.	33
4.4. Analysis techniques.....	35
4.4.1. FTIR (Fourier Transform Infrared Spectroscopy)	35
4.4.2. DSC (Differential Scanning Calorimetry)	37
4.4.3. Thermogravimetric analysis (TGA).....	42
4.4.4. Scanning electron microscopy (SEM).....	42

4.4.5.	Impedance spectroscopy (IS)	44
4.4.6.	Data treatment software	45
5.	Results and discussion	46
5.1.	FTIR results obtained in the analysis and evaluation.....	47
5.2.	DSC results obtained in the analysis and evaluation	50
5.2.1.	Heating	50
5.2.2.	Cooling	51
5.3.	TGA results obtained in the analysis and evaluation.....	53
5.4.	SEM results obtained in the analysis and evaluation	55
5.4.1.	Fiber diameter measurements and analysis.....	59
5.5.	IS results obtained in the analysis and evaluation.....	61
5.5.1.	Impedance modulus (R) analysis.....	61
5.5.2.	Impedance phase (ϕ) analysis	63
5.5.3.	Capacitance and dielectric constant analysis	64
6.	Regulatory framework	68
6.1.	Property rights	68
6.2.	Safety measures.....	68
7.	Socio-economic environment.....	69
7.1.	Project's budget	69
7.2.	Future applications and research impact	69
8.	Justification of the solution and conclusions.....	70
9.	References	71

1. Abstract

Main objective of this work is the preparation and characterization of polymer nanocomposites with potential electric properties. Nanocomposites are based in Ethylene-vinyl acetate (EVA) with copper (Cu) nanoparticles.

Materials are prepared using Solution Blow Spinning. This fabrication process is an innovative method to produce micro- and nanofibers, which are woven forming a mat. It consists in targeting a rotating collector with polymer-nanoparticles composite solution using an air-brush. The different techniques are employed to study the properties of these materials. Fourier transform infrared spectroscopy (FTIR) analysis will provide structural information. Thermal properties are determined by differential scanning calorimetry (DSC) and thermogravimetric analysis (TGA). Scanning electron microscopy (SEM) represents the sample morphology. Finally, electrical properties of the samples were studied undergoing an impedance spectroscopy (IS). These analyses were run for the different concentrations of Cu nanoparticles established (0%, 2% and 5% wt).

The addition of Cu nanoparticles showed no change in structure of the nanocomposites according to the results obtained in FTIR analysis. Analysis done by DSC didn't show variations in thermograms between different concentrations of Cu nanoparticles, moreover the inclusion of them help slightly to improve the thermal resistance shown by TGA analysis. The treatment of SEM images presented, fibers with a diameter in the order of nanometers and a great dispersion of Cu nanoparticles was achieved. To conclude, IS analysis showed a reduction on the impedance (Z) if the percentage in weight of Cu nanoparticles increases and thus greater capacitances were found. Moreover, percolation threshold was not reached, opening a path of improvement.

2. Introduction and objectives

This work is object of new creation polymeric nanocomposites which have unknown morphology, physical, thermal and electrical properties. Polymer nanocomposites are known for the enhancement of its properties with respect to conventional nanocomposites. Additionally, less quantity of material is able to deliver same or better performance in mechanical stress tests and thermal analysis [1]. Polymer nanocomposites are reported to have a uniqueness behavior. The surface-to-volume ratio makes the difference between other materials. Techniques like Solution Blow Spinning, object of this project, allow the homogeneous dispersion of nanoparticles in the polymeric matrix. The inclusion of certain nanoparticles has reportedly improved the electrical properties of the polymers and also thermal ones [2].

Nowadays the use of thermoplastic matrix nanocomposites has great interest, one of the common thermoplastic polymer used is EVA, due to its physical properties which vary without a required phase change. EVA is the polymer used for the purpose of enhancement of its electrical properties. The predictions of how certain polymer nanocomposites will behave are almost impossible. Empirical methods are used to present its properties. The problem raised is the enhancement of the electrical properties of EVA polymer nanofibers by the inclusion of different concentrations of Cu nanoparticles. The inclusion of Cu nanoparticles provides a twist of the screw by approaching the electric behavior of the nanocomposite to a more capacitive material. On the contrary, EVA nanofibers approach to a more insulating behavior [3].

One of the novel techniques to produce nanocomposites in form of fiber was developed since 1902, when John Francis Cooley patented the first modern process of electrospinning, but the research before that patent started in the seventeenth century [4], [5]. Electrospinning technologies and the so called, melt blowing governed as the method of creation of polymeric nanofibers, but the 27st of April 2009 when Eliton S. Medeiros published an article with the description of a new technique alternative to those ones stated which was called Solution Blow Spinning and was able to produce polymeric nanofibers. This kind of fabrication process will be wide explained in chapter 3 [6].

2.1. Objectives

2.1.1. General approach

The principal objective of this work is obtaining new polymer composite materials with potential electrical properties.

2.1.2. Specific goals

Control and learn the technique of Solution Blow Spinning and the preparation of solutions mixtures of EVA/Cu with different concentrations of Cu nanoparticles.

- Production of EVA-Cu nanocomposite using SBS
- Study the possible filler effect in the properties and morphology of the EVA: Characterize the materials prepared undergoing the following analysis:
 1. Structure: Fourier transform infrared spectroscopy (FTIR)
 2. Thermal properties: Differential scanning calorimetry (DSC) and Thermogravimetric analysis (TGA)
 3. Morphology: Scanning electron microscope (SEM)
 4. Electric behavior: Impedance Spectroscopy (IS)
- Discover and conclude the effect that the different concentration of Cu nanoparticles makes to the nanocomposite EVA/Cu properties specifically in the electrical behavior.

3. Fundamentals

Just to clarify, there are some definitions that everyone should be willing to know before the start of the explanation of the experiment. These concepts are summarized in the following topics:

3.1 Polymer Composite Materials

- Nanocomposites

3.2 Composites with electrical properties

3.3 Ethylene-vinyl acetate (EVA) Copolymers

3.4 Cu nanoparticles

3.5 Fabrication process

- Solution Blow Spinning (SBS)

3.1. Polymer composite materials

Composites can be characterized as materials that comprise of at least two synthetically and physically unique stages isolated by an unmistakable interface. The distinctive frameworks are consolidated wisely to accomplish a framework with more helpful basic or useful properties unattainable by any of the constituent alone. Composites, the superb materials are turning into a basic piece of today's materials because of the favorable circumstances, e.g., low weight, corrosion resistance, fatigue strength, and fast assembly [7]. Applying those concepts to the nanocomposites field require a miniaturization of the materials, till nanometer scale. The nanometer is a metric unit of length and means one-billion of a meter or 10^{-9} m. Famously, nano is additionally utilized as a descriptive word to portray items, frameworks, or marvels with attributes emerging from nanometer-scale structure.

In nanometric order of magnitude, nanostructured materials are found. They first appear with the current development of the field of nanotechnology. Many existing materials are organized on the micro- scale and nanometer scales, and numerous mechanical procedures that have been utilized for quite a long time e.g., polymer and steel fabricating use nanoscale materials, also in the electronic and computer field. The requirements to distinguish nanomaterials are mainly dimension type. They are materials that have auxiliary parts with a size less than $1\ \mu\text{m}$ in no less than one dimension. While the nuclear and sub-atomic building squares (0.2 nm) of matter are considered nanomaterials, cases, for example, materials with dispersing cross section of nanometers however plainly visible measurements are generally rejected [8].

3.1.1. Polymer nanofibers

A nanofiber is a nanomaterial in perspective of its distance across (diameter), and can be viewed as a nanostructured material if loaded with nanoparticles to frame composite nanofibers, which is the case of this experiment.

Additionally, nanofibers are characterized as filaments with distance across less than 1000 nm. There are different procedures for polymeric nanofiber creation, for example, the ones previously stated like meltdown blowing, electrospinning and the one object of this project, Solution Blow Spinning (SBS) [9].

3.2. Composites with electrical properties

Composites materials are researched with different aims, mainly the enhancement of physical and structural properties but also its chemical ones and electrical properties. In particular, polymer composites have been recently object of enhancement of its electrical properties. The applications and possibilities are huge, i.e. anti-static materials, electromagnetic interference shielding, chemical sensors. Normally polymer composites are filled with micro or nano-sized particulate matter which enhances electrical conductivity as its concentration rises.

The conductive properties are explained by the percolation theory. This theory states that the inclusion of conductive fillers inside the polymer could form conductive pathways generating transitions from insulating to conductive. The concentration required of conductive filler to occur the transition is called the percolation threshold. Most common fillers used are: Carbon Nano Tubes (CNT), Copper (Cu), Aluminum (Al), Nickel (Ni) or Steel (Ag) [2].

3.3. Ethylene-Vinyl Acetate (EVA) Copolymers

In this work, the copolymer Ethylene-Vinyl Acetate (EVA) is object of Solution Blow Spinning technique. First, in order to understand the experiment, it should be clarified some definitions:

- Monomer: it is a molecule, which is joined to other molecules normally by covalent bond and is able to undergo a process of polymerization, which consists in the transformation of a monomer or a mixture of them into a polymer.
- Polymer: it consists in macromolecules (normally organic) formed by the union of covalent bonds between one or more simple units called monomers.
- Copolymer: they are species obtained from more than one monomer macromolecules. They are generated by the process of copolymerization, a process in which a copolymer is created [10].

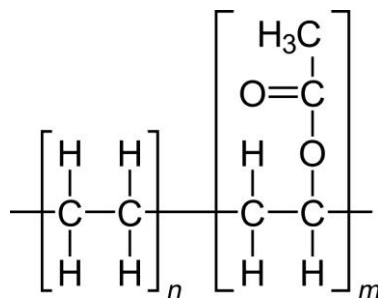


Figure 1. Chemist structure of EVA

Ethylene-Vinyl Acetate (EVA) is a thermoplastic polymer formed by Ethylene and Vinyl Acetate units (Figure 1). EVA copolymers are utilized broadly in the wire and link industry for making heat shrinkable protection, semi-conductive protection coats, and fire-resistant protection. The main ethylene copolymers, including EVA, were orchestrated and protected in the 1930s at IC1 in Great Britain in similar labs where polyethylene was found.

At first, just low levels of vinyl acetate derivation co-monomer were utilized to create "changed polyethylene". During the late 1950s and proceeding to the present day, the scope of EVA copolymers has augmented significantly, mirroring a gratefulness for the flexibility of the material. Today the expression "EVA copolymer" covers a various group of materials, which for the motivations behind in this project a 40% by weight of vinyl acetic acid derivation is used.

In fact, EVA copolymers are used in maybe the broadest range of uses of any manufactured polymeric material. Vinyl acetate has two central impacts that affect the properties of EVA copolymers. The main impact is to disturb the crystalline zones shaped by the polyethylene fragments of the copolymer. Low and medium thickness polyethylene, created by the high-weight mass process normally show degrees of crystallinity in the scope of 40-65% as analyzed by X-ray diffraction and affirmed by differential scanning calorimetry (DSC). This is continuously lessened by expanding VA content until, eventually in between of 40 and 50 wt% VA, the material turns out to be totally indistinct.

The capacity to change the level of crystallinity of semi-crystalline EVA copolymers has been of preeminent significance in controlling properties for specific end utilities and is to a great extent in charge of the unparalleled adaptability of these items. The absolute most critical properties controlled partially by the level of crystallinity are recorded in Table 1, as a component of expanding vinyl acetate content, for example, a diminishing crystallinity.

Table 1. Changes in physical properties of EVA as a function of decreased crystallinity due to increasing Vinyl Acetate content [11].

Stiffness modulus	Decreases
Surface hardness	Decreases
Crystalline melting point/softening point	Decreases
Tensile yield strength	Decreases
Chemical resistance	Decreases (generally)
Impact strength (especially at low temperatures)	Increases
Optical clarity	Increases
Gas permeability	Increases
Environmental stress crack resistance	Increases
Coefficient of friction	Increases
Retention of mechanical strength at high fibre loadings	Increases
Compatibility with other polymers, resins, etc.	Variable

The second impact of vinyl acetate outcomes from the polarity of the acetoxy side chain. In this manner, as the vinyl acetate builds, so does the polarity of the copolymer. Albeit maybe less tremendous and clear than the decrease in crystallinity, this expansion in polarity additionally offers ascend to various fascinating and imperative properties that are once more, to some degree, in charge of the wide differing qualities of utilizations for EVA copolymers. Some of these properties are recorded in Table 2 with a sign of the heading in which the property changes with expanding VA content [11].

Some of the most common applications of EVA Copolymer are:

- Wire and Cable Insulation
- Bundling Film/Coextrusion Layers
- Adhesives/Paper Coatings
- Cover Backing
- Trim and Extrusion
- Foam
- Sound Damping/Sound Barrier Sheet
- Solar cell encapsulant

Table 2. Changes in physical properties of EVA related to increased polarity due to increasing Vinyl Acetate Content [11].

Dielectric loss factor ($\tan \delta$)	Increases
Compatibility with polar resins and plasticizers	Increases
Specific adhesion (in adhesive formulations)	Increases
Printability (ability to accept printing inks)	Increases

3.4. Cu nanoparticles

Nanoparticles are particles with no less than one dimension with a size less than 1 μm , and possibly as little as nuclear and atomic length scales (0.2 nm). A nanoparticle can also be a zero-dimensional nanoelement, which is the most straightforward type of nanostructure. Nanoparticles can have indistinct or crystalline frame, and their surfaces can go about as bearers for fluid beads or gasses. To some degree, nanoparticulate matter ought to be viewed as an unmistakable condition of matter, notwithstanding the solid, fluid, gaseous, and plasma states, because of its particular properties large surface range and quantum confinement effects (describe electrons in terms of energy levels) [8], [9].

Recent studies have seen colossal development, because of the uncommon chemical and physical properties, which have been shown to be a middle of the road state of matter. The catalytic activity (substance that boost the reaction rate without adjusting the general standard Gibbs energy change) of the particles by and large relies on upon their size, shape, and balancing out conditions, which are controlled by the planning conditions [12]. There are various ways to deal with the planning of the nanoscale materials, some of these techniques incorporate controlled chemical lessening, electrochemical reduction, and metal vaporization [13].

Copper is an imperative material due to its high electrical and warm conductivities. Nanoscale materials in different structures, for example, one-dimensional, crystal, center shell, and inside empty structures, are preferably suited for an extensive variety of utilizations in science and industry for its great optical, catalytic and optical features [14]. X-Ray Diffraction has shown that Cu colloids tend to react with the oxygen from the environment and leads to its oxidation, transforming Cu nanoparticles in Cu_2O [15]. Cu_2O and CuO are known as p-type semiconductors showing slender band gaps and have been broadly utilized as capable catalysts. For instance, Cu_2O has an immediate band hole (2.0 eV), which makes it a promising material for obtaining electrical and chemical energy from a solar source [14]. Its morphology and its rounded shape help to the formation of clusters (Figure 2).

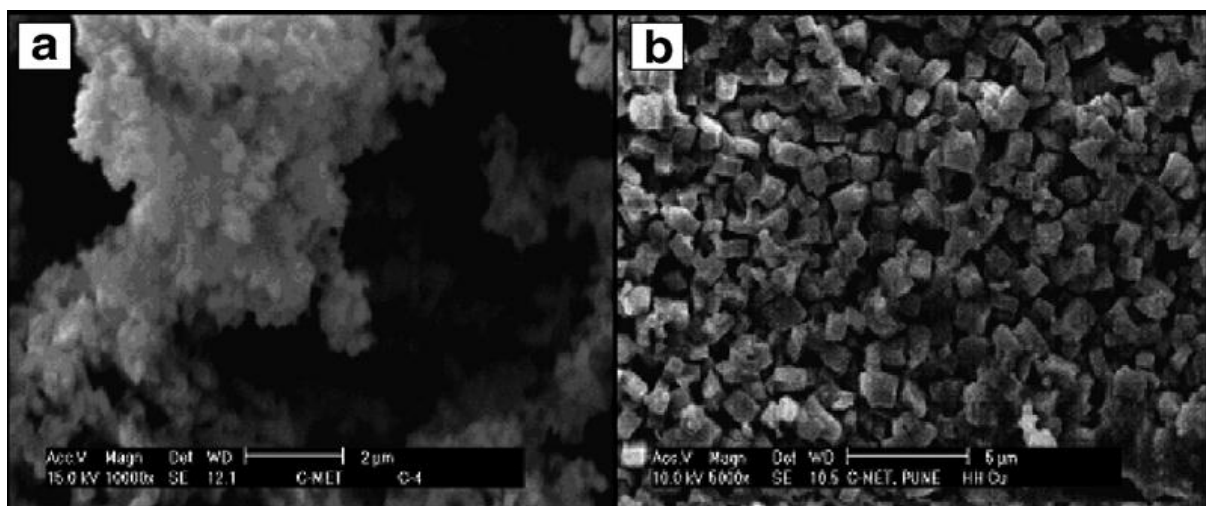


Figure 2. SEM images of (a) myristic acid capped nano-Cu, (b) Cu/PVA nano-composite [15].

3.5. Fabrication process

3.5.1. Origin and common methods to generate polymeric nanofibers

In the eighteenth and nineteenth century, George Mathias Bose stated the utilization of sprays that created electric potentials to droplets of liquids. The nineteenth century, Louis Schwabe improved the manufacturing process of creation of fibers. He performed experiments using ductile techniques and fine holes were used by Schwabe. At the end of this century, in 1892, Jodrell Laboratories located near London, developed a new technique to create cotton thread, which delivered a glossy finish. The method was improved with the invention of the Topham Box by Charles Topham, which allowed the fiber to be gathered on a bobbin.

Finally, in the twentieth century, John Francis Cooley created a machine that could be considered the first modern electrospinning process. In his patent called "Apparatus for electrically dispersing fluids" published in 1899 describes a process in which he used four types of spinning heads. It combines the action of high tension electricity that generates an electric field and the projection of composite fluids. The fibers generated are wrapped around a reeling mechanism [4]. There were other famous contributors such as Anton Formhals, who published a total of 22 patents improving the electrospinning method. He ended up controlling the production of shorter fibers.

At the second half of the twentieth century, the electrospinning acquired a continue development till the day of today, which can be considered an industrial process. Some limitations are found in the electrospinning process, such us low fiber production efficiently and the solvent compatibility with this process, because of the influence of the solvent's dielectric constant [6].

The other alternative to solution blow spinning for a method to create polymeric fibers is melt down blowing. This process consists of a melted polymer jet that is conducted through a stream of transporter gas to produce fibers. There is a drag force exerted by the gas that disperses the fibers and create them, but not only that, it also cools them. The process is limited by two constraints, there's only possible to use thermoplastic polymers and the method is not able to produce fibers within a size range, like electrospinning does [16]. The origins of this process are found in the middle of the twentieth century, when Van A. Wentz, who worked for the Naval Research Laboratories, tried to measure the radiation in the atmosphere with the purpose to evaluate nuclear weapons behavior. To achieve that, he thought about the creation of fibers that absorb the radiation and in the creation, process he used the concept of meltblowing [17].

Pooling the knowledge used for the techniques previously mentioned, Solution Blow Spinning (SBS) technique was recently developed by Eliton S. Medeiros at the beginning of 2009 as an alternative to the existing methods of electrospinning and melt blowing techniques of creating micro and nanofibers from polymeric solutions. This new technique combined elements from both techniques [6].

Solution Blow Spinning technique is based on solution spinning, which has been used since 19th century as a method to create polymeric fibers. This process works as an airbrush, solved polymer travels through slim holes of a spinning nozzle, fibers are extruded and the solvent used removed. Fine fibers are created, which have a reduced fiber diameter and an improved mechanical strength.

Solution Blow Spinning process is composed by several determining elements, such as a syringe flow injection rate, pressure of the gas injected, working distance, solvents used and solution concentration. Those elements determine the output obtained.

3.5.2. How Solution Blow Spinning works?

Solution Blow Spinning is a process that generates polymer nanofibers. It consists in a syringe pump that injects a polymer solution at a constant flow rate into a nozzle, where this mixture and pressurized air arrives. Both fluids are not mixed inside, but in the output of the nozzle they touch each other [6].

Air arrives with a greater pressure, P_1 , than the atmospheric pressure, P_{atm} , which generates a pressure difference, $P_1 - P_{atm} = 0.5$ bar capable of generating an air jet, which is expanded (Figure 3). The air jet exerts a force in the polymer as it comes out from the nozzle. Then the fibers are elongated and they travel for 20 cm till the collector, a sufficient distance for the solvent mixture to evaporate just leaving the EVA nanofiber. This generates a drag force on the gas solution boundary provoked by tangential forces exerted on the mixture. The forces elongate the dissolved EVA generating fibers and the fibers arrive at the collector, where they are spinned.

The Solution Blow Spinning technique uses the Daniel Bernoulli's equations collected in his book called "Hydrodynamica (1738)". A compressor is connected through a pipe to the output, where atmospheric pressure is found. The pressure-drop occurred in the pipe is what accelerates the air and it creates a piping air system. Analyzing this model is quite complex, since there are few unknown characteristics of the system, like the dynamic viscosity, friction factor, Reynolds number or the volumetric rate of air, although a theoretical approach can be done [18].

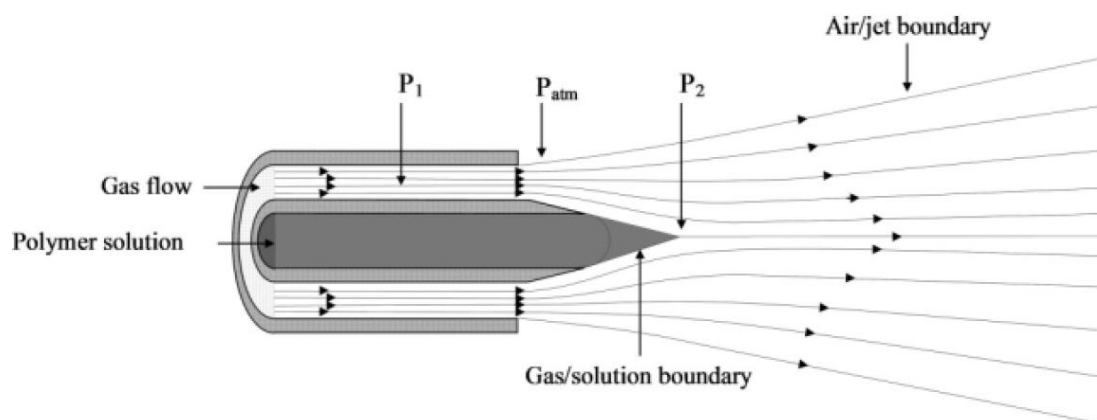


Figure 3. Nozzle's output schema.[6]

3.5.3. Theoretical approach to Solution Blow Spinning process

Air thrust lengthens and stretches the solution, while also the solvent mixture evaporates. In order to give a theoretical approach to how this model behaves a Dripping Faucet model is followed.

The Dripping Faucet model represents how does a water stream flowing from a tap (same direction as gravity acceleration) behaves depending on its flow rate (Q). This is also based on the Daniel Bernoulli's equations. In concrete, the continuity equation:

$$A_1 v_1 = A_2 v_2 \quad Q_1 = Q_2$$

Where A_1 is the area of the stream at the outlet of the nozzle and A_2 is the area of the stream when it changes its phase from liquid state to solid. v_1 is the starting stream velocity and v_2 is the final velocity reached when all the solvent is evaporated (Figure 4).

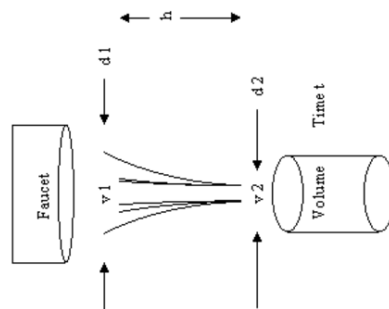


Figure 4. Model of a simple case of a Dripping Faucet.

In the Dripping Faucet model the gravity acceleration does not vary, but the flow rate does. The model concludes that when the flow rate is greater the water stream breaks into drips at a higher distance and when it is low, it can start dripping (Figure 5).

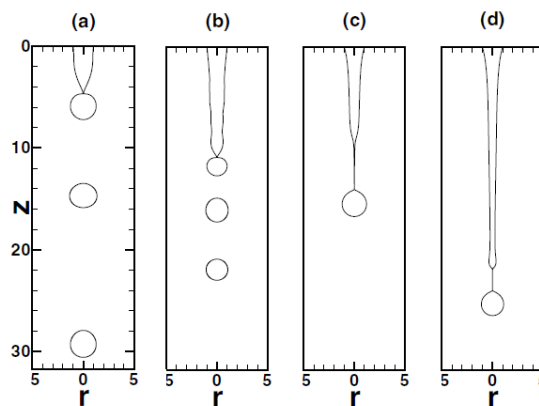


Figure 5. Water streams from a) lowest flow rate till d) highest flow rate [19].

Reworking the model to our Solution Blow Spinning technique. Gravity can be neglected, because the air thrust exerts a much greater force on the flow stream. The acceleration increases the velocity and as the continuity equation states, the polymer-solvent mixture stream surface decreases to a point where the cross section has an order of nanometers.

- Common mistakes in SBS found

Dripping: as an analogy to the Dripping Faucet model, it can happen that the nozzle outputs just polymer globs. If the globs arrive the collector, it might be that the pressure difference between the compressor and the atmosphere is high enough to brake the polymer mixture stream before the solvent is evaporated leaving $A_2 \approx 0$. A decrease in pressure difference can be a solution and the variation of the flow rate. If the globs are formed at the output, the pressure difference might increase.

The fiber diameter can be predicted, moreover there are few other conditions that affect the final fiber diameter, which are not object of this project and are difficult to determine to build a precise model.

Moreover, to build a model able to predict future behavior of other polymers, polymer type and polymer concentration in the mixture are the most crucial factors.

4. Experimental part

Since, it is already explained how the technique works, now according to the article: "Solution Blow Spinning: A new method to produce Micro- and Nanofibers from Polymer Solutions". It is going to be clarified point by point, how it is performed [6].

So, in this project, the objective is the creation of EVA/Cu Nanoparticles Nanocomposites in order to characterize them and study its potential electrical applications. Since, there are no records or other articles, where researchers have analyzed this behavior. It is going to be performed three different experiments and the comparison between them will provide an overall view about the results obtained.

The technique that is going to be used is Solution Blow Spinning. Before, it was explained the apparatus needed to perform the experiment, now it is going to be explained the methodology and the results obtained.

Previously, to the explanation, the characteristics of the commercial EVA used, Cu nanoparticles, and solvents used (Chloroform and Dichloromethane) are shown.

4.1. Materials

4.1.1. Commercial EVA

In this case, it is used Poly (ethylene-co-vinyl acetate) with a 40% in weight of Vinyl Acetate. It has the following properties:

Table 3. Properties of commercial EVA [20].

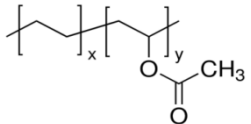
Poly(ethylene-co-vinyl acetate)	
Linear Formula	$(\text{CH}_2\text{CH}_2)_m[\text{CH}_2\text{CH}(\text{OCOCH}_3)]_n$
Form	Beads
Autoignition temperature	260 °C
Melt index	57 g/10 min (190°C/2.16kg)
Contains	200-800 ppm BHT as inhibitor
Composition	vinyl acetate, 40 wt. %
Hardness	40 (Shore A-2, ASTM D 2240)
Transition temperature	$T_g = -40 - -30 \text{ }^\circ\text{C}$ $T_m = 110-120 \text{ }^\circ\text{C}$
Solubility	toluene, THF, and MEK: soluble



Figure 6. EVA bottle from Sigma Aldrich brand.

In the following graph appears a representation of the FTIR (Fourier transform infrared spectroscopy), where the composition of EVA can be appreciated:

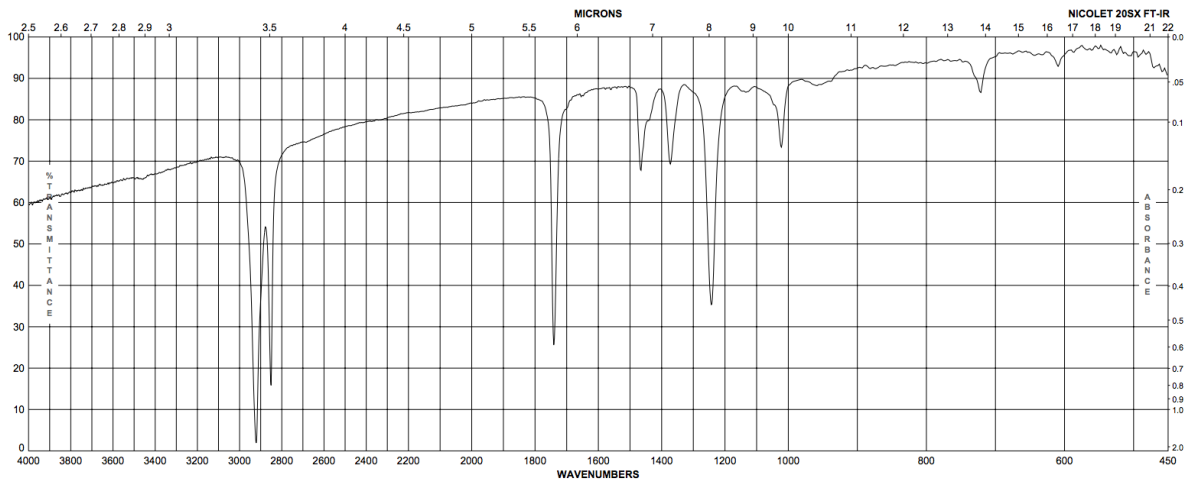


Figure 7. Commercial EVA transmittance [21].

In the next figure appears the inside of the bottle of Poly(ethylene-co-vinyl acetate) from the manufacturer Sigma-Aldrich (Figure 8). It can be appreciated beads inside.



Figure 8. EVA beads.

4.1.2. Solvents

Chloroform

It is one of the solvents used, it was provided like the EVA by Sigma-Aldrich. As a main feature, it has 99% of concentration and has the following properties:

Table 4. Properties of Chloroform [21].

Empirical formula	CHCl_3
Molecular Weight	119.38
Grade	Anhydrous
Vapor density	4.1 (vs air)
Assay	$\geq 99\%$
Contains	Amylenes as stabilizer
Impurities	0.005% water (100mL)
Evapn. residue	$<0.0003\%$
Color	Colorless
Bp	60.5-61.5 °C(lit.)
Mp	-63 °C(lit.)
Density	1.48 g/mL at 25 °C; 1.492 g/mL at 25 °C(lit.)

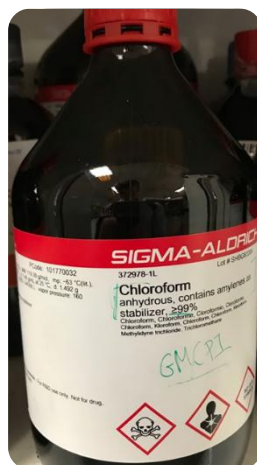


Figure 9. Chloroform bottle from Sigma Aldrich brand.

Dichloromethane

It is the other solvent used, it was provided again by Sigma-Aldrich. As a main feature, it has 99.8% of concentration and has the following features:

Table 5. Properties of Dichloromethane [21].

Empirical formula	CH ₂ Cl ₂
Molecular Weight	84.93
Grade	Anhydrous
Vapor density	2.9 (vs air)
Vapor pressure	24.45 psi (55 °C); 6.83 psi (20 °C)
Assay	≥99.8%
Autoignition temperature	662 °C
Contains	40-150 ppm amylene as stabilizer
Impurities	0.005% water (100mL)
Evapn. residue	<0.0005%
Bp	39.8-40 °C(lit.)
Mp	-97 °C(lit.)
Density	1.325 g/mL at 25 °C(lit.)

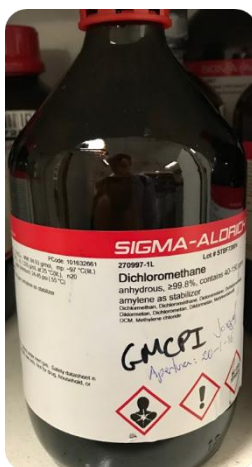


Figure 10. Dichloromethane bottle from Sigma Aldrich brand.

4.1.3. Cu nanoparticles

Copper Nanoparticles were used since the focus of this experiment is the study of the electrical behavior of EVA/Cu nanocomposite. They were provided by a company called Hongwu International Group Ltd.

Table 6. Properties of Cu nanoparticles [22].

Particles size	70 nm
Purity	99,99 %
Package	100 g



Figure 11. Cu nanoparticles bag from Hongwu International.

4.2. Fabrication process

4.2.1. Elements of the SBS equipment

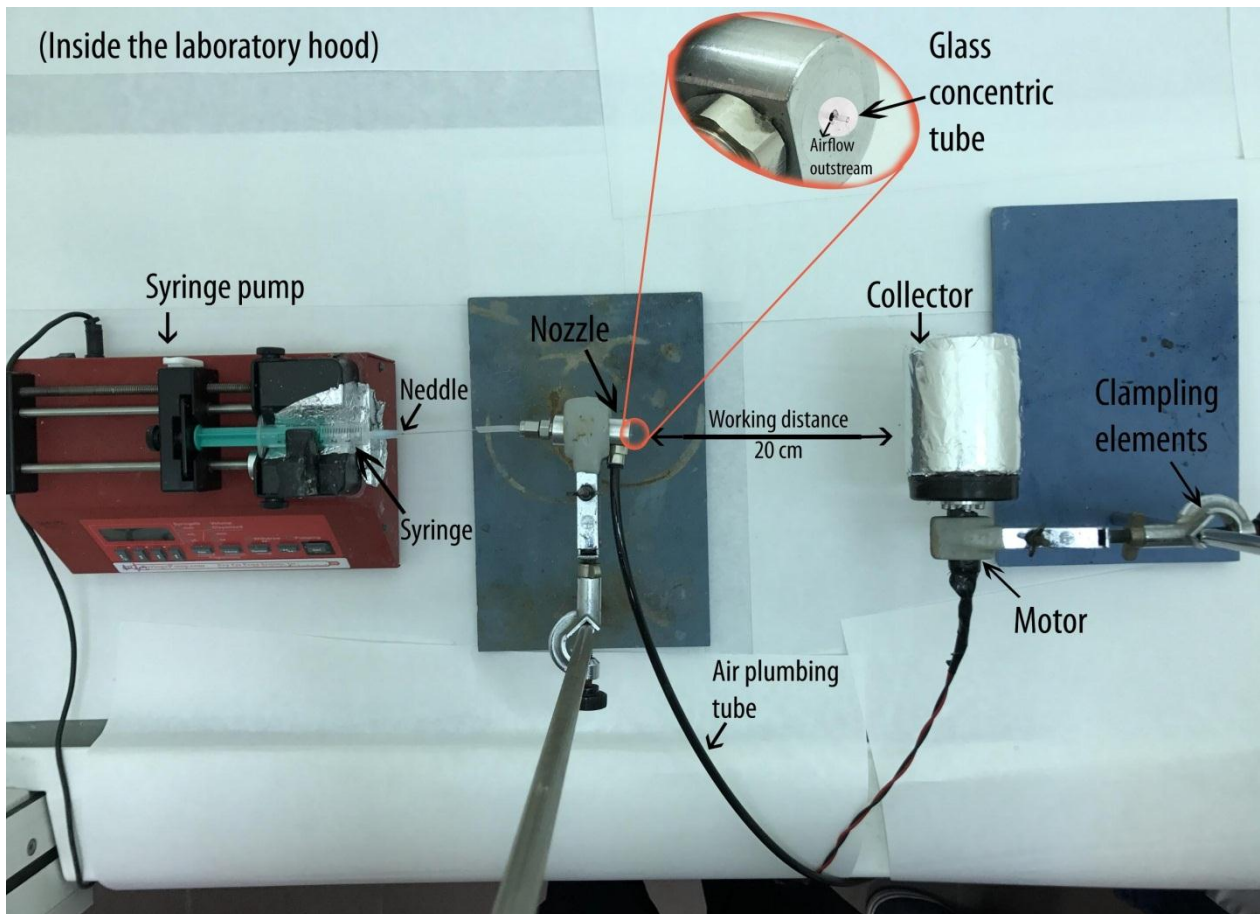


Figure 12. Actual set up used for SBS in the laboratory. The different elements are named in the image.

Each part of this equipment is explained as follows:

Syringe pumping system

The syringe pumping system is a simple apparatus, which allows the user to control the injection rate of the dissolved polymer which is piped. The model used is New Era Pump System Inc. NE-1010. The pumping system allows us to set precise values of flow rate in several measurement units. When the flow rate is selected, the syringe pump is ready and pressing the start button a compressing plate exerts force in the plunger top and the dissolved polymer is piped through the needle. In this project, the unit used is mL/min.

Syringe

A commonly used syringe is valid for the injection of the solved polymer. In this particular case, the syringe pump used a 10 mL standard syringe. The syringe is attached to the pumping unit and

secured by a rotating top plate; this provides stability and doesn't allow the syringe to be moved even when the machine exerts force.

Needle

A needle is joined together with the syringe in the adaptor. It is important to make sure that no solvent is spilled out of the needle and the needle is not obstructed. The bevel of the needle is introduced in a small plumbing tube.

Plumbing tube

The needle is inserted into a plumbing tube, made out of silicone and this tube comes from a nozzle. The insertion of the needle into the tube must be done taking into account that no fluid should be spilled and the sharp bevel cannot puncture the inner part of the tube or the flow of solved polymer can be obstructed.

Air compressor

An air compressor is used in order achieve a determined pressure conditions, that are willing to obtain the best results in the creation of nanomaterials. In this project, a large compressor is used. The apparatus is composed by a big tank, where air is inserted; when the compressor is plugged the machine is ready to work. A pressure gage displays the pressure that the instrument should achieve. The pressure value is controlled by a rotating wheel, since the moment the compressor is powered on the motor inserts air till it reaches the pressure desired and then it stops.

A valve, right next to the pressure gage, there is a pressure valve, which opens and closes the output of air. The pressure taken into account is the one that the pressure gage shows when the release valve is open. The model used was NU-AIR OL2-50 CE.

Air plumbing tube

A dark colored tube made out of polyurethane is plugged into the output of the release valve. The polyurethane tube must be able to withstand high pressures. In the installation should be checked that there's no drain, otherwise the pressure delivered is not precise.

Nozzle

This part is where the pressurized air and the solved polymer arrive in their respective silicone tubes. Inside, the two fluids flow separately. They are conducted till a tip, where a small hole communicates with the outside. In this hole, a concentric tube made out of thin glass is placed. The glass tube is where the solved polymer is going to be released; in particular the tip is located ahead of the end of the nozzle (protruded 2 mm), which facilitates the thrust caused by the air. The two fluids are not mixed inside the nozzle. The solved polymer flows inside the glass tube and the air outside, until it reaches the outside.

Collector

The collector is located at a determined distance from the tip of the glass tube. This distance is called working distance and should be set. The collector is composed by a round plastic vial, which is cut in four sections leaving a gap where it is formed the fiber's mat. This helps to collect the material. The vial is screwed and has a motor attached, that spins at constant velocity.

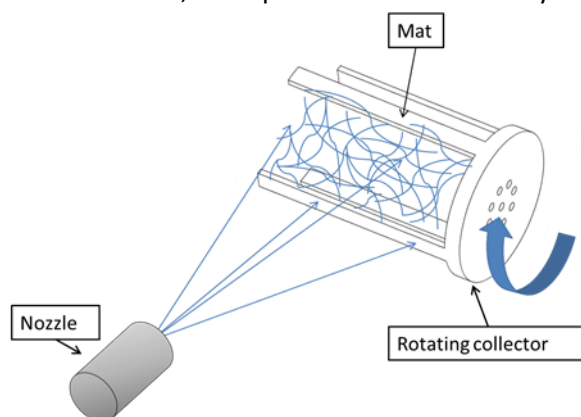


Figure 13. Schema of how the collector looks like and the gap where the mat is formed.

Motor

The motor is attached to the collector, to make it rotate at a constant speed. It must be plugged and has a switch. The motor rotates at a speed of 270 rpm.

4.2.2. How to perform an experiment?

To perform an experiment, it is followed a set up procedure.

1. The polymer solution should remain stirred, while the apparatus is set up. A magnetic stirrer helps with this task. The magnetic stirrer is a tool that creates a rotating magnetic field, which causes the spinning of a stir bar, which was previously introduced inside the vial. These machines have two adjustable parameters: spinning speed and temperature (heat).

In the Solution Blow Spinning experiment, there's no need of heating, because the solvents used are quite volatile at ambient temperature (25°C). The evaporation of the solvent causes a variation in the molar fraction of the polymer in the mixture.

2. The syringe pump is plugged in and configured with the desired injection velocity in mL/min.
3. Two syringes are needed: one for clean-up, that is not needed to be replaced and another one, which will be pumped and contains the polymer solution. This syringe must be replaced each time that, an experiment is performed to assure, that it has the conditions previously stated and there's no waste. Before and after an experiment, it is cleaned pumping two syringes of acetone.

4. The needle is introduced inside the plumbing tube connected to the nozzle without making any damage to the interior with the bevel.
5. The air plumbing tube is connected to the nozzle, the air compressor plugged in and the working pressure set. The motor starts working and when it is filled, stops.
6. The clamping elements are mounted, making sure that the high of the nozzle fastened is the same as the collector one.
7. The collector is attached using the clamp; the motor plugged in and located at a determined working distance.

Opening the valve of the compressor, pressing the button to start pumping the material dissolved and powering on the motor to make the collector spinning starts the experiment.

4.2.3. Optimization phase

Previous to the analysis, an optimization process has been performed by the by the GMCPi research group of the Department of Material's Science in UC3M. This process has the objective to obtain the best working conditions for the Solution Blow Spinning's Apparatus in order to obtain fibers. In this project, this part hasn't been covered. Since there was no background in the optimization of the generation of EVA nanofibers using the SBS technique, it was needed to perform an analysis to determine the best possible conditions using SBS process. The analysis consists in a trial and error process till it is found the best working conditions to develop the project. The conclusions obtained at the end of this part are explained in the next section.

4.3. Sample preparation

Three different samples are prepared for further analysis. What varies between them is the concentration of Cu nanoparticles.

- EVA with 0% in weight of Cu nanoparticles
- EVA with 2% in weight of Cu nanoparticles
- EVA with 5% in weight of Cu nanoparticles

4.3.1. Solution preparation

Solutions were prepared one day before the experiment. The main reason why it should be done the previous day to the experiment is because of ensuring the completely dissolution of polymer in the solvents.

Starting with the process, since toxic solvents (chloroform and dichloromethane) are used, safety measures must be considered. Before beginning we must make sure that we have in hand the following tools:

- Vial with a plastic cover
- Stir bar
- Commercial EVA beads bottle
- Chloroform bottle
- Dichloromethane bottle
- 2x syringes with needles attached to the tip, one for chloroform and the other for dichloromethane
- Laboratory spoon
- Laboratory tweezer
- Parafilm
- Electronic balance

The process is described in the following steps and it belongs to EVA-Cu 0%.

1. The electronic balance is taken and cleaned with a brush to remove chips and dust, we don't want any effect from external agents. The windows that cover the balance are closed and the balance is tared (is set to 0 grams).
2. The vial is introduced with the stir bar inside. The stir bar must be cleaned using acetone. The weight is annotated in grams. The precision of the electronic balance is quite high (10^{-4} grams), but as the last digit changes so much, a precision till milligrams (10^{-3}) is taken.

3. After that, using the laboratory spoon and carefully the EVA beads are introduced. In concrete 1.05g of commercial EVA. After introducing the polymer, the weight is noted.
4. In the next step, we need to wear the breathing mask and protecting goggles because we are going to operate with the solvents, Chloroform and Dichloromethane. As it is known the optimized conditions for the Solution Blow Spinning process when producing EVA nanofibers, the percentage in weight (w) of EVA is 7% and EVA's weight used is 1.05g. So, the 93% left is constituted by the solvents mixture, in concrete doing a simple proportion is 13.95g. In our experiment, 50% in weight of 13.95g is used of each solvent: 6.975g of Chloroform and 6.975g of Dichloromethane. After, we know the quantity to operate; it is extracted from the bottles of the respective solvents using one syringe to manipulate each solvent. Then, carefully one of the syringes is spilled inside the vial with EVA till the specific mass is introduced. Then, rapidly (the solvent volatilizes fast) and we do not want to lose the precision in the concentration of EVA. Then, it is closed with the plastic cover and covered the top with parafilm. The remaining solvents in the syringes are carefully returned to the respectively bottles. To conclude the total weight, of the mixture is 15g.
5. When it is finished, we collect all the tools and store the solvents. The vial will remain for one day till EVA is dissolved in a cool environment avoiding heat and shield with the plastic cover and parafilm.

In the cases of EVA with inclusion of Cu nanoparticles changes a little the solution preparation process. The following steps differ for the case of EVA-2% Cu and EVA-5% Cu:

4. In the next step, we need to wear the breathing mask and protecting goggles because we are going to operate with the solvents, Chloroform and Dichloromethane. As it is known, the optimized conditions for the Solution Blow Spinning process when producing EVA nanofibers, the percentage in weight (w) of EVA is 7% and EVA's weight used is 1.05g. So, the 93% left is constituted by the solvents mixture, in concrete doing a simple proportion is 13.95g. In this case, two vials are prepared. In the first vial, EVA and the stir bar are introduced. In total, it is needed a concentration in weight of 7% with respect to the solvent mixture. In this vial, just 5.23125g of each solvent is introduced (10.4625g in total), the concentration is greater but the remaining 1.74375g of each solvent is leaved for the second respecting the concentration of 7% when both vials are merged together. A greater quantity of solvents is introduced in this vial with respect to the other one, because it is needed that EVA is properly dissolved in the Chloroform and Dichloromethane mixture.
5. After, we know the quantity to operate; it is extracted from the bottles of the respective solvents using one syringe to manipulate each solvent. Then, carefully one of the syringes is spilled inside the vial with EVA till the specific mass is introduced. Then, rapidly (the solvent volatilizes fast) and we do not want to lose the precision in the concentration of EVA. Then, it is closed with the plastic cover and covered the top with parafilm. The remaining solvents in the syringes are carefully returned to the respectively bottles.

6. The second vial is where Cu nanoparticles are introduced. Different weight is introduced depending on the percentage in weight desired, which is presented in Table 7 and calculated using Equation 2. Moreover, the quantity of each solvent is 1.74375g (3.4875g in total) in both cases. Cu nanoparticles are also toxic and can enter our body by respiratory tracts, therefore safety measures are needed like when handling with solvents. The Cu nanoparticles are extracted using the laboratory spoon and carefully inserted in the vial. After that, the solvents are included using the respective syringes and the vial is shield using the plastic cover and parafilm.

$$\text{Weight of Cu nanoparticles}(g) = \frac{\text{mass of EVA}(g)}{\% \text{ of Cu nanoparticles} / 100} \quad \text{Equation 1}$$

Table 7. Weight in grams of the different concentrations of Cu nanoparticles.

Sample	2% of Cu nanoparticles	5% of Cu nanoparticles
Weight (grams)	0.021	0.055

When it is finished, we collect all the tools and store the solvents. The vials will remain for one day till EVA is dissolved in a cool environment avoiding heat and shield with the plastic cover and parafilm. The result obtained is shown in Figure 14:



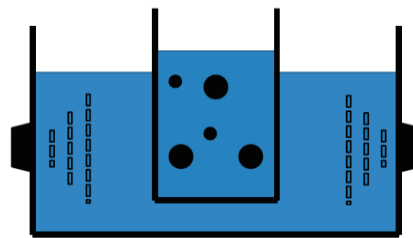
Figure 14. On the left, EVA vial with the magnetic stirrer inside and on the right-side Cu vial is found.

The reason why one specific vial for the Cu nanoparticles is needed is because Cu nanoparticles are attached between them and they form clusters (group of particles joined together). In Solution Blow Spinning, the objective is to disperse the Cu nanoparticles homogeneous in the EVA fibers generated, to solve this situation Cu nanoparticles should remain in an ultrasonic bath for 30 minutes approximately before Solution Blow Spinning is performed.

Ultrasonic bath of Cu nanoparticles

Ultrasonic bath or sonication is referred to the process where sound energy at high frequency (more than 20 kHz) and normally inaudible to the human ear is used in order to disperse and disrupt agglomerates of particles, i.e. Cu nanoparticles, undergoing a process called cavitation. It is said that this process is more energy efficient and the degree of fragmentation of the nanoparticles dust is greater than other dispersion methods [23]. Cavitation phenomena consists in shock-wave generation, jetting and broadband acoustic emissions that have been used as a mechanical trigger with different purposes, such as industrial or medical ones [24].

A nanoparticle is considered a primary particle, normally between 1 and 100 nm. Agglomerates or aggregates are considered a union of primary particles. These particles are normally bonded together for different reasons, such as mechanical bonding, sintering or foundry and it is difficult to split them. Normally, between them are exerted relatively weak forces, like electrostatic ones or Van der Waals forces. To separate the agglomerates, the Cu nanoparticle's vial will undergo a process of sonication for 30 minutes. The Figure 15 represents a schema of the process. In the center and semi-submerged in water is the vial placed.



Bath

Figure 15. Ultrasonic bath [23].

Ultrasonic disruption consists mainly in two processes. The first one, in the low-pressure cycle (rarefaction) is formed microscopic vapor bubbles, through cavitation. Then a high-pressure cycle starts. The frequencies normally alternate between 20 kHz (low pressure) and 40 kHz (high pressure). The high-pressure cycle compresses the vapor bubbles and produces a shock-wave that releases a tremendous amount of mechanical and thermal energy (the water, where the vial is submerged, increases its temperature). As, our vial shielded is in suspension in water, the process is called indirect sonication and sound waves must travel through the water and the vial's wall and liquid [23].

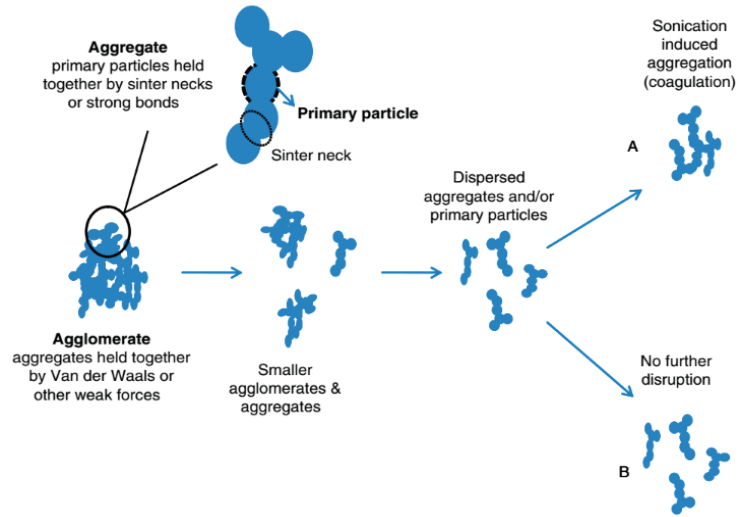


Figure 16. Schema about the process of disaggregation [23].

4.3.2. Films preparation. Working conditions

First of all, Solution Blow Spinning technique has different working conditions that affect the output obtained from the apparatus. The working conditions are parameters that could be changed in order to get a specific result. The working conditions seem to be not unique and there is the possibility of finding several ones, which will generate fibers with different diameters [6].

Polymer type

The type of polymer that undergoes SBS process has the greater effect on the gathering of fibers. In our case, it is used Poly (ethylene-co-vinyl acetate) with 40% of vinyl acetate.

Polymer concentration

This parameter is the concentration of EVA in the solvent mixture. It is measured in percentage of weight. In this work 7 % by weight was used in the solvent mixture. So, the mixture of solvents was in a 5:5 proportion of weight of Chloroform and Dichloromethane. On the other hand, the solvent's evaporation rates during the process can influence the fiber formation, for this reason solvents with low boiling point are excellent choice for this process.

Injection rate

The injection rate is the flow rate in which the syringe pump pipes the dissolved polymer through the tubes. In our case, it has a constant flow rate of 0.25 mL/min. This rate is enough slow to produce the "extrusion" of the solution drops. The injection rate has a range of possible values in which fibers are generated. In other analysis performed to other polymers it is observed that a variety of injections rates are valid.

Gas flow pressure

The gas flow pressure is the output pressure from the air coming from compressor from the outer nozzle. It is measured in Bar and in our case, it was set at 0.5 bar. This pressure is adequately low to remove the solvent at the same time drop extrusion, which leads to fiber production.

Working distance

The working distance is how far is the collector set from the edge of the concentric tube made of the nozzle made from glass, where the dissolved polymer comes out. The working distance of the experiment was set at 20 cm. Just to clarify, the height at where the collector is settled and the height of the concentric glass tube of the nozzle have to be the same. The reception is perpendicular to the output of the nozzle. This working distance is perfect to remove all solvent during the fiber flight [6].

4.3.3. Films preparation. Experiment.

First of all, the system is cleaned using acetone/air syringes. The flow rate is set at around 5 mL/min and the pressure conditions between 2 bar and 4 bar. These causes the acetone and air to eject with more force, removing the impurities easily.

The safety measures will be used again during the experiment. The process is done inside the laboratory hood while is off, if not the fibers would fly upwards and we want that they go perpendicular to the collector. The vial is placed in the magnetic stirrer leaving it in movement. The syringe pump is set to 0.25 mL/min and the pressure of the air stream to 0.5 bar.

This process has the following steps:

1. We take a syringe and we take about 4 mL of EVA mixture.
2. The motor is powered on and the syringe is placed and attached to the syringe pump. The release valve is open and the pressurized air flows.
3. The forward button is pressed in the syringe pump system and the polymer solutions start to come out slowly lasting 16 minutes. The collector gathers the polymer fibers.



Figure 17. Polymer mat created by undergoing SBS at the before mentioned working conditions.

The collector has like a polymer web around. With the help of scissors, it is cut and left in an aluminum paper sheet. The remaining dissolved EVA is used to prepare the sample of FTIR analysis and to perform the second mat of polymer fibers.

In the films that include 2% and 5% of polymeric nanofibers the process is the same as before, just leaving the vials 30 minutes in the sonifier before the start of the experiment. It was used Fisherbrand Ultrasonic Unit. It was established that our vials have to remain about 30 minutes in the sonifier apparatus. The vial should stay in suspension in the water and not completely submerged. Sonification process heats up the water and as it is said before our solvents are volatile at ambient temperature, so if the temperature is increased significantly the pressure inside increases and can

cause an aperture of the cover and an evaporation of the solvent mixture. To avoid this situation the water of the sonifier should be changed frequently (almost each 5 minutes). Our concrete sonifier used has a maximum frequency of 37 kHz [24]. The apparatus includes a drain that can be open and decreases the water level of the sonifier. In Figure 18 is represented how the particles solution is sonicated.



Figure 18. EVA/Cu mixture vial undergoing an ultrasonic bath for 30 minutes.

4.4. Analysis techniques

4.4.1. FTIR (Fourier Transform Infrared Spectroscopy)

The use of infrared spectrometry is mainly used in the polymer laboratories as a primary instrument to determine the molecular structure of the composite. The analysis provides information, which is unreachable by other approaches.

The way FTIR spectrometry analysis measure infrared spectrum is because the vibrational energy states are measured. These vibrations go from a simple diatomic molecule vibration to a complicated movement of atoms in a large molecule. In molecule that has N atoms there are $3N$ degrees of freedom, they are called modes. So, if a molecule has 6 degrees of freedom has 6 atoms that have harmonic displacements oscillating at a determined frequency that is characteristic. These frequencies are measured using the units of cm^{-1} . The mid-infrared spectrum ($400 - 4000 \text{ cm}^{-1}$) is where most of the vibrating modes' frequencies are located. The analyses performed in our experiment are set between those frequencies.

Normally, most of the molecules are almost fixed, but some molecules have large movement and displacements. Those modes belong to a concrete functional group and it is not affected by other atoms in the molecule. With FTIR spectrometry we are capable of matching an infrared spectrum of vibrational modes with specific functional groups. This shows the possibility to assign specific chemical functional groups to certain frequencies. The Colthup charts are glossaries, where there is the possibility to assign specific absorption bands to functional groups. Every molecule has different vibrating modes from another. The sample used needs to be at about $10 \mu\text{m}$ of thickness to run a good analysis in the mid-infrared spectrum. The bands cannot be saturated requiring a transmittance of less than 1% [25].

Our polymer in the FTIR is attached to Potassium Bromide cell manufactured by us. The cell is a circle of approximately 1 cm of diameter, where the polymer should be sticked. The Potassium Bromide cells are transparent to the infrared light and they do not introduce lines or interferences in the spectra.

FTIR analysis is performed using a FTIR spectrometer. The apparatus is connected to a computer which manages and controls the parameters of the scanning process. The samples are introduced in an attachment made of carton which places the sample in the center of the transmitter infrared beam. The IR source travels through the sample and arrives at the detector. FTIR generates wavelengths from a range between 400 and 4000 cm^{-1} , which are absorbed partially by the sample identifying the functional group. The FTIR scanner is controlled by a computer by the software Spectrum v2 with the following parameters presented in Table 8.

Table 8. Configuration parameters of FTIR analysis.

Interval	Resolution	Nº of scans	Range
$0,5 \text{ cm}^{-1}$	2 cm^{-1}	20	$400 - 4000 \text{ cm}^{-1}$

The data obtained in our FTIR analysis is the absorbance which consists in the quantity of light absorbed by the sample. The opposite parameter that is also used is the transmittance, which consists in the energy that the sample can transmit.

The FTIR analyzer used is from the manufacturer Perkin Elmer and in concrete the model Spectrum GX (Figure 19).

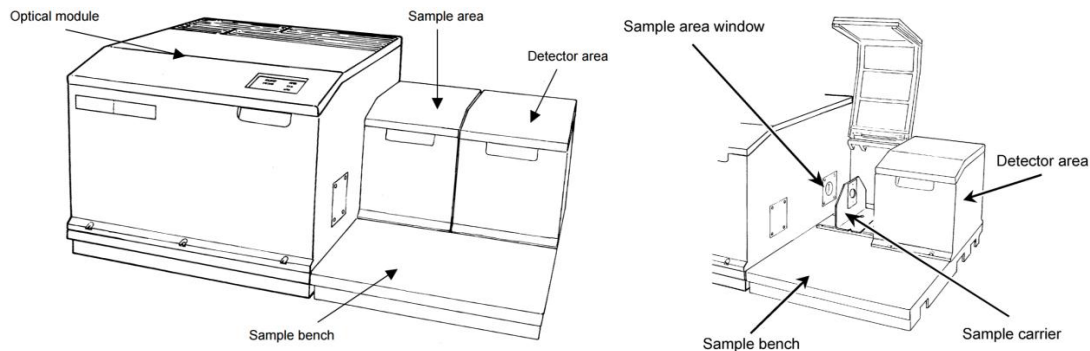


Figure 19. Schema of the FTIR apparatus used. The sample carrier is where the potassium bromide cell is attached to perform an analysis [26].

How to prepare the Potassium Bromide (KBr) cells?

In order to prepare the cells used to analyze samples in the FTIR spectrometer, the Potassium Bromide cells are needed. Those rounded cells can be bought or can be manufactured. In our case, they are going to be manufactured. As it is seen in the photo, Potassium Bromide is a salt that comes in a dust form. This salt is crushed using a small mortar and pestle and is compressed with a small manual pneumatic press it is compressed. To fabricate one cell, it is needed about 0.2 grams of Potassium Bromide, and then it is mashed and introduced in the pneumatic press. This press is set to exert a pressure of 7 tons and with the Potassium Bromide inside a lever is pulled. It leaves a cell that can be transparent to our eyes and so it is to infrared spectrum used in the FTIR spectrometer.



Figure 20. On the left shows the pneumatic press with the lever on his right side. The right picture shows the placement in the electronic balance of KBr.

Since solution blow spinning targets with polymer fibers a certain boundary region, we have to make sure that it points directly to where the cell is. The cells are attached to a thick glass plate with double sided tape and with the help of a ruler, they are placed using the same working conditions. Just 1 mL of mixture is used to prepare the samples. As it was previously stated, if more material was utilized the thickness would cause later in the FTIR analysis would produce a saturated result and if it has a low thickness the signal would be so low and useless.

4.4.2. DSC (Differential Scanning Calorimetry)

Differential Scanning Calorimetry analysis is a technique that is based in calorimetry. The technique measures heat, which means the heat exchanged. A heat exchange causes a variation in temperature of a sample, which wants to be analyzed. The local change in temperature differences provides the ability to measure the heat flux. With the data collected and studied, Differential Scanning Calorimetry provides crucial information about chemical reactions and physical transitions that can occur in the sample. These changes are directly connected with the consumption and generation of heat.

Based on DSC technique for this project Differential Thermal Analysis (DTA) is utilized. The difference lies in the application of temperature differences between a sample to be analyzed and a reference sample as function of temperature or time. DTA shows the heat exchange qualitatively. It is just needed a small sample with a small relative mass in the order of milligrams. It has a wide range of temperatures, which the apparatus can reach almost the absolute 0 Kelvin. The accuracy of the equipment is high.

There are a few types of DSC equipment; the one object of this project belongs to the Power Compensation DSC class. This type is a heat-compensating calorimeter. Heat measured is compensated increasing or decreasing an electric resistor Joule's heat. In Figure 21 is shown a schematic of DSC equipment. It corresponds to the small furnace that DSC has, it can maintain a constant temperature. S indicates Sample and R indicates Reference. Number 1, corresponds to the heating wire and Number 2, to a resistance thermometer.

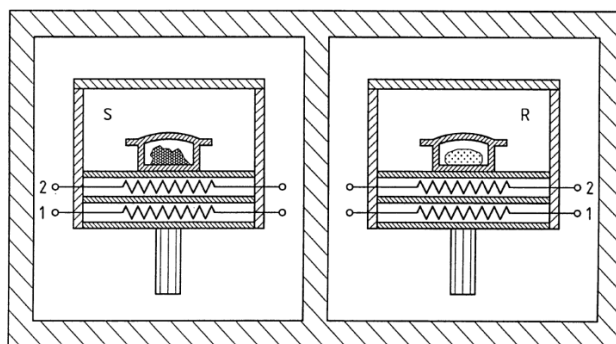


Figure 21. Represents a schema of the Sample furnace on the left and the Reference furnace on the right.

This type of DSC apparatus has the ability to reach low temperatures, such as - 175 °C with the help of liquid nitrogen cooling and maximum temperatures of 725 °C. Furthermore, in the next Figure 22 is shown a schema of how the apparatus obtains results:

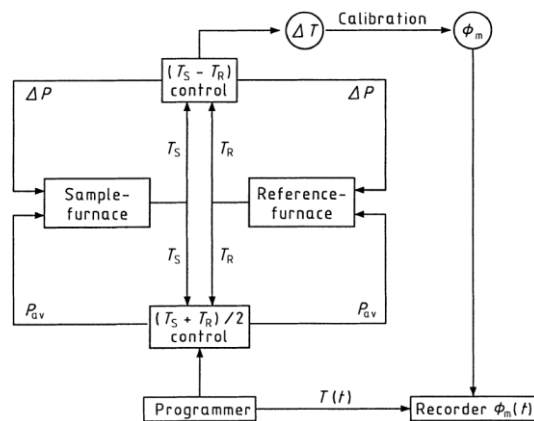


Figure 22. Schema of calculations done by DSC apparatus.

As explained before, the machinery has two furnaces and it performs a programmed study by an operator (in this case us). This study consists in a variation of temperatures during a certain amount of time. So, if both furnaces during the undergoing of the process remain at an ideal constant temperature, it indicates a thermal symmetry (both vials stay at same temperature). In the other hand, when a thermal asymmetry occurs (the temperature is not the same in the sample and the reference) means that a reaction to heat in the sample has occurred.

DSC uses this temperature difference as a signal to be processed. The apparatus reacts to this difference varying the heating power in order to compensate the reaction heat flow to maintain the same temperature between the Sample and the Reference furnace. An increment of Power (ΔP) is obtained, which is proportional to the remaining temperature increment (ΔT). Performing an integral to the compensating heating power over the time leaves Q_r , a heat consumed or discharged by the sample. At the end, a manufacturer-set calibration process undergoes correcting the data and obtaining the heat flow rate (Φ_m) [27].

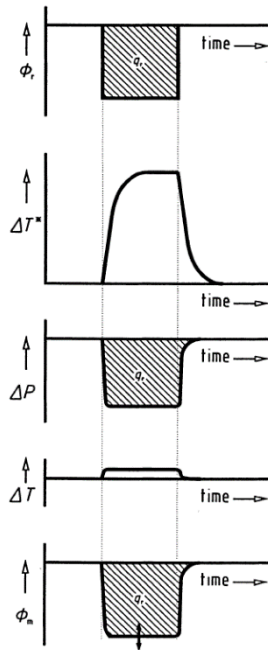


Figure 23. Example of a compensation in which the temperature of the sample furnace increased more than in the reference furnace. DSC apparatus decreased its heating power and applying its manufacturer corrections the heat flow rate (Φ_m) was obtained.

Heat power compensations during the time deliver a final plot of graph of the heat flow rate versus the duration time. These results are obtained for the three different samples object of this project.

How to prepare the samples?

The two furnaces are called by the manufacturer, Mettler Toledo, aluminum crucible. They have a capacity of 40 μL , which is quite small. The needed samples are from the order of 4 to 5 milligrams. The base is flat and the crucible shallow, which to minimize the creation of possible gradients. While the process runs, the temperature increases so does the pressure inside. To avoid a crucible opening a hole is done on the lid (upper part of the crucible). The hole can be done with a simple needle to both the Sample and the Reference.



Figure 24. The crucible used (left) and the crucible press (right).

Table 9. Mass used in DSC analysis.

EVA 0% Cu nanoparticles	EVA 2% Cu nanoparticles	EVA 5% Cu nanoparticles
4,5 mg	4,6 mg	4,4 mg

Table 10. Crucible dimensions and weight.

Weight	Height	Diameter
2 grams (approx.)	6 mm	9 mm

To prepare the samples for the DSC analysis, Mettler Toledo, provided a crucible sealing press. It is an apparatus that exerts a small amount of pressure to shield the crucibles that are used for DSC. The action of a lever while the sample is in the press is enough to attach the lid (cover). The mass used for each sample (Table 9) should be provided to DSC software to perform the thermograms.



Figure 25. Inside of the DSC furnace.

Figure 25 shows the inside of the furnace. As stated before, it is appreciated the two samples inside their respective furnaces (S, Sample and R, Reference). When loaded with the sample and the reference a glass, metal covers it. It helps to maintain a constant temperature inside the small cavity, which is very important for the analysis [28].

The DSC model used was manufactured by Mettler Toledo. DSC822e Differential Scanning Calorimeter (DSC) is the concrete model which belongs to the Power Compensating DSC type and has a sensor plate that guarantees great sensibility, robustness and resolution. The next Figure 26 shows the outside of the apparatus.



Figure 26. Mettler Toledo DSC822e (DSC).

Operation with DSC and thermogram characteristics

Mettler Toledo Differential Scanning Calorimeter uses a software provided by the manufacturer which is called STARe [29].

1. The first step is to define a temperature profile that the sample should follow. The range of temperature of this DSC goes from -150 °C (just with a Nitrogen Cooling System) to 700 °C with a maximum heating speed of 100K/min (with a 400W source). The profile followed is the next one (Figure 27):

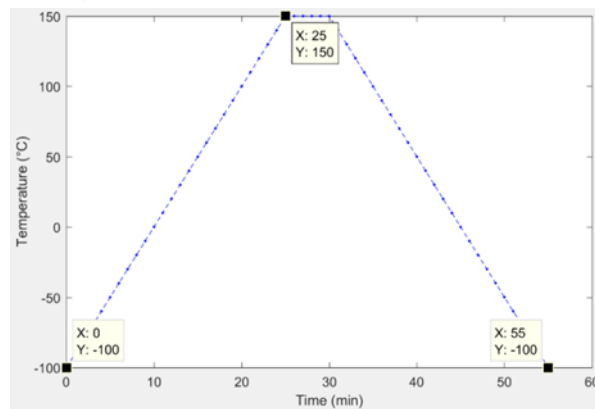


Figure 27. Temperature profile followed in DSC.

2. The apparatus uses a Nitrogen Cooling System (to be able to achieve -100 °C) and runs in an inert atmosphere of nitrogen gas, N₂.
Nitrogen Cooling System is composed of a liquid nitrogen tank which is attached to the back of the DSC using a valve. The valve can set a certain output pressure, which is defined between 1 and 1.5 bar.
The analysis runs in an inert atmosphere of N₂, which means that the sample doesn't react with the atmosphere. Other gases can be used, such as oxygen (O₂) but in that case, won't be an inert atmosphere. This is useful for certain purposes, i.e. carbon reaction with oxygen, but it is not our case.
The nitrogen gas cylinder is connected to the DSC and has a release valve that can control the flow rate, which according to the manufacturer should be 80 mL/min (30 psi).
After setting those conditions, the process can start.
3. When the profile to study is defined, the DSC is turned on. It is connected to a computer which needs to run STAR software to communicate with the DSC unit. The Reference and our Sample are placed in the sensor using tweezers. We must be careful as the sensor is quite delicate. Then, the glass cover is fixed. Using STARe the profile is loaded and the experiment sent.
4. DSC will go to the start temperature (in our case -100°C) and when it arrives, STARe will give the possibility to start with the analysis. In our case the analysis last 55 minutes and has to be performed for each of the samples.

5. When it finishes, the software delivers a graph with the results obtained. The samples are removed and DSC reset. N₂ gas cylinder and liquid nitrogen tank valves are closed. DSC is turned off and the software closed [29].

4.4.3. Thermogravimetric analysis (TGA)

Thermogravimetric analysis (TGA) is a process which consists in the measurement of mass changes while the samples object of study varies its temperature under a profile followed. Normally, the temperature variation changes at a constant rate.

The apparatus used is called thermo balance, which is an electronically programmed furnace capable of reaching more than 1000 °C. The process undergoes under a static or a dynamic atmosphere at a determined flow rate of a gas which can be inert, like nitrogen and helium or reactive, like oxygen. In this project, all analyses were run in an inert atmosphere of N₂ a constant flow rate of 20 mL/min. The heating rate used was 10 °C/min.

The measurements took place in the thermo balance TGA-SDTA 851 Mettler Toledo in the Department of Chemistry of the University of Navarra. The samples are introduced in the furnace in melting pots with a capacity of 70 µL.

4.4.4. Scanning electron microscopy (SEM)

For research purposes in the field of nanomaterials, the observation of the morphology is quite important. The method of scanning electron microscopy is widely used nowadays and helps to understand this field. This technique was invented by Ruska and Knoll back in 1931.

Scanning electron microscope produces an electron beam generated by a source which is targeted to a probe. The incident electrons follow a matrix scanning path, which is represented in Figure 28. The interactions between the probe and the electron beam generate distinct types of emitted electrons which are registered by different sensors.

The apparatus can work in two diverse ways, one can display the morphological shape of the sample and the second one is able to interpret its composition. The electron beam in the first case emits secondary electrons, which are electrons with energies smaller than 50 eV and in the second case, backscattered electrons are emitted whose energies are more than 50 eV. Secondary electrons (SE) produce mainly inelastic collisions while back scattered electrons (BSE) produce elastic ones. The number of back scattered electrons dispersed increases with greater atomic numbers and thus appear in SEM images brighter as high atomic number elements are examined. In the images obtained, it is able to recognize, where the Cu nanoparticles are placed [30].

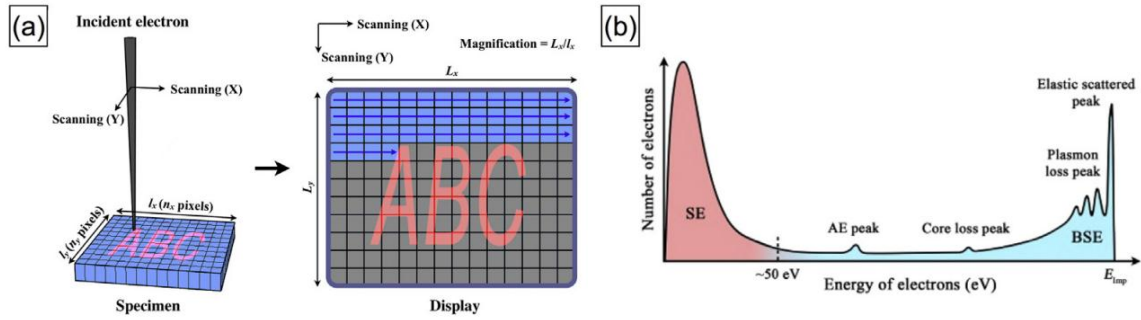


Figure 28. Electron beam and how the apparatus does its scanning process [30].

SEM images are in black and white represented. In the case of secondary electrons (SE), brighter areas correspond to a greater number of SE detected by the sensors. In the case of BSE, as the collisions are inelastic, the sensor which is different from the one for SE, brighter areas will correspond to high atomic composition.

For this project, the microscope used is the Phillips XL30. The analyses were done from x250 till x5000 augmentations for the three concentrations of Cu nanoparticles. The samples, before being analyzed by the microscope are prepared using a technique called sputtering. The sputtering process was first patented in 1974, by John S. Chapin. In this project, it is used a sputtering coating using gold often applied to poorly conducting materials, such as polymers. The gold coating helps to prevent the charging of the sample, phenomena that could be caused by the accumulation of electric fields (Figure 29). It enhances the detection by the microscope of secondary electrons and improves the beam resolution [31]. The time of gold sputtering was 1 min.

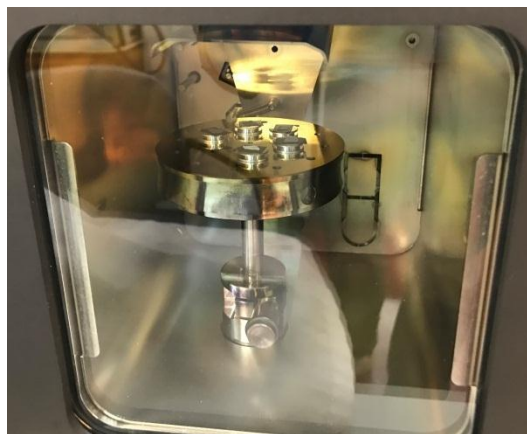


Figure 29. Sputter apparatus with the samples attached. The process undergoes in vacuum and plasma is created. The machine is from the manufacturer Leica.

4.4.5. Impedance spectroscopy (IS)

The impedance spectroscopy was carried out by a frequency response analyzer. It is an apparatus patented first in 1962 and is able to measure the electrical properties of electrical networks and its frequency response, which is represented in logarithmic scale [32], [33].

It generates a phase modulated signal which is addressed to the sample under test. The output signal is delivered in two channels, which are multiplied by a reference signal and its product is integrated. These apparatuses are composed by several elements, such as multipliers, integrators, phase modulators or function generators. The actions of those elements are combined to form a correlator, whose signal is multiplied by the two reference functions; sine and cosine sifted 90 degrees. Then, the values are integrated and a waveform is obtained, which is then extracted the polar coordinates (angle and modulus).

The mathematical expressions that the apparatus follow are the following:

$$\frac{a}{2} = \frac{1}{NT} \int_0^{NT} R \sin(\omega t + \phi) \sin \omega t dt = \frac{1}{2} R \cos \phi \quad \text{Equation 2}$$

$$\frac{b}{2} = \frac{1}{NT} \int_0^{NT} R \sin(\omega t + \phi) \cos \omega t dt = \frac{1}{2} R \sin \phi \quad \text{Equation 3}$$

NT is the number of cycles whose waveform's period is T.

$$R = \sqrt{a^2 + b^2}; \phi = \tan^{-1}\left(\frac{b}{a}\right) \quad \text{Equation 4}$$

In equation 5, a term corresponds to the resistance (r), real term and the imaginary term (b), which corresponds to the reactance. Frequency response analyzer is able to obtain the impedance in polar coordinates, as well as its modulus (R) and argument (ϕ). For the case of this project, those values were represented as a function of the frequency ($f = 1/T$) obtaining at the end a waveform of the impedance's modulus and argument as a function of the frequency. It was represented in logarithmic scale.

The impedance varies depending on the concentration and is dependant of sample's thickness, increasing as long as the sample thickness is incremented. In order to elaborate a conclusion, thickness measurements were done. It was used a precise electronic caliber from Mitutoyo brand. The frequency response analyzer used was the 1260 Impedance/Gain-Phase Analyzer by Solartron analytical. To perform this study the home-made device was used (Figure 30). It is formed by two Poly(methyl methacrylate) plates, which are fixed using two bolts and nuts. In between, there are two rounded plates where the samples are introduced and fastened. Then, two wires cables are fixed to the two conducting plates. The two wires are connected to the frequency response analyzer and the test can be run.

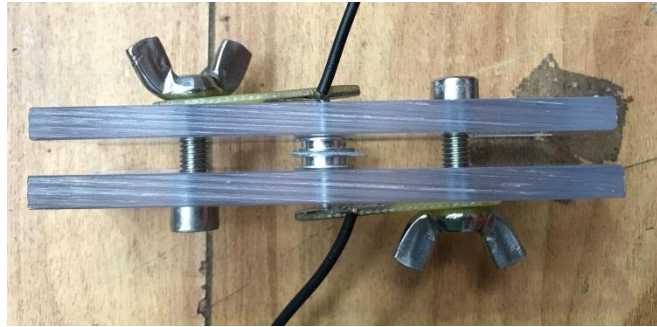


Figure 30. Device to test samples with the FRA.

Thickness measurements

The evaluation of the electric behavior required measurements of the thickness of the sample. Using the thickness, it is possible to compute the capacitance and the dielectric constant. Measurements were done using a precise digital micrometer presented in Figure 31. Results are shown when the electric behavior is analyzed.

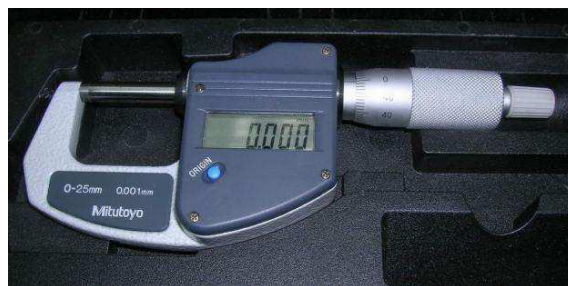


Figure 31. Digital micrometer used.

4.4.6. Data treatment software

Different software was used to treat and picture the data obtained in the previously explained analysis.

OriginPro is a data analysis and graphing software of choice for over a large portion of researchers and architects in business ventures, the scholarly community, and government labs around the world. Origin offers a simple to-utilize interface for learners, joined with the capacity to perform propelled customization as you turn out to be more acquainted with the application. It was used for graph plotting, statistical analysis and data representation. For this purpose, it was also used the well know MATLAB software, which can handle complex impedances obtained from the Impedance Spectroscopy (IS) analysis.

ImageJ is an image processing tool which has the possibility to measure areas, angle and distance between pixels. In the software, a scale is defined with a certain magnitude and the program transforms a concrete number of pixels, defined by the user, to measurements in the selected scaling. It has statistic features also. It was used in to measure fiber diameter from SEM images.

5. Results and discussion

At this point and with an experimental part finished, it is obtained three samples:

- EVA 40% with 0% in weight in Cu nanoparticles
- EVA 40% with 2% in weight in Cu nanoparticles
- EVA 40% with 5% in weight in Cu nanoparticles

In order to obtain a conclusion and discuss the results obtained, a series of analysis will be performed:

- FTIR (Fourier Transform Infrared Spectroscopy)
- DSC (Differential Scanning Calorimetry)
- TGA (Thermogravimetric analysis)
- SEM (Scanning electron microscope)
- IS (Impedance spectroscopy analysis)

These analyses help to characterize the material obtained, how is their behavior electrically and thermally, its composition and morphology.

5.1. FTIR results obtained in the analysis and evaluation

FTIR spectrometer delivers data of the structural information of the samples. The absorbance bands show the functional groups, which the sample contains. As a first approximation, the next Figure 32 shows the spectra of the samples depending on its concentration. To obtain this approach Origin statistical software was used and a baseline was established.

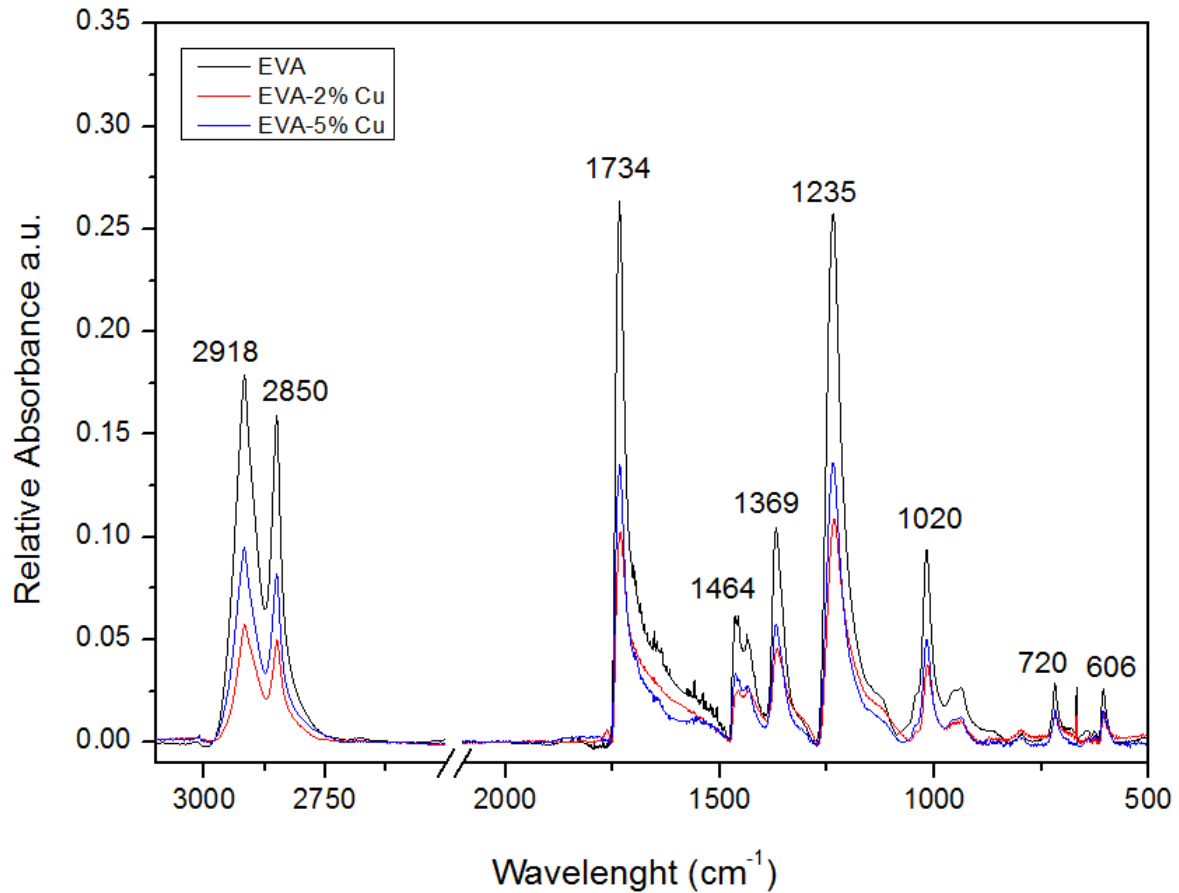


Figure 32. Spectrum of the absorbance of the three samples obtained in FTIR analysis.

It can be appreciated that the samples have peaks of absorbance in the same wavelength, but it seems that there is difference in the absorbance levels. Absorbance is an optical effect which is thickness dependent. Beer-Lambert Law states that an increase on film thickness will raise the concentration of material which is tested. It follows the following mathematical expression, Equation 6:

$$A = \sum_{i=1}^N A_i = \sum_{i=1}^N \epsilon_i \int_0^l c_i(z) dz \quad \text{Equation 5}$$

ϵ_i : absorptivity

c_i : concentration of the material sample

l : distance that light travels through the material. [34]

To compare the samples, thickness of the film deposited in the Potassium Bromide cells is difficult to measure and use Beer-Lambert Law. As an approximation using Origin software the wavelengths are normalized and it is obtained a relative absorbance of the samples, which is represented in the next Figure 33:

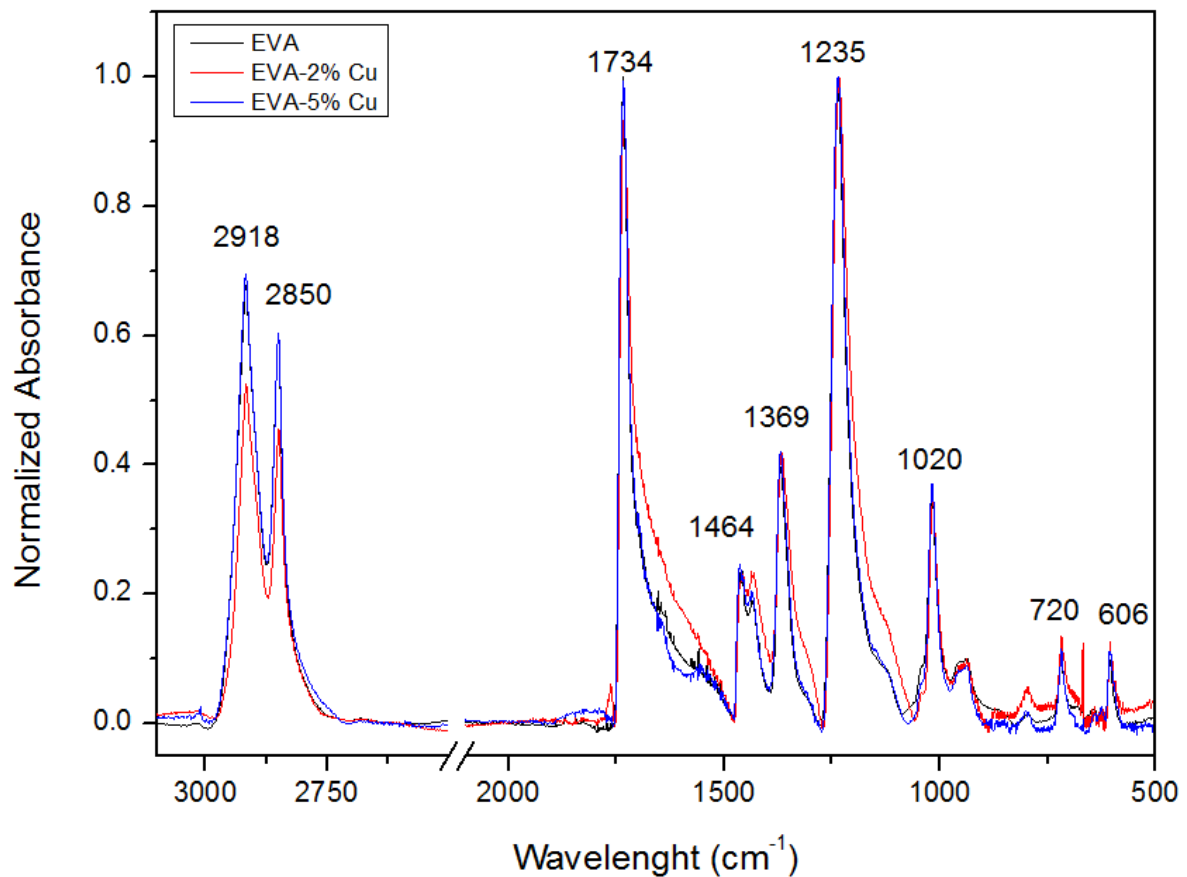


Figure 33. Plot of the normalized absorbance (applying the dividing by its maximum technique).

So far, it is observed that the inclusion of Cu nanoparticles has not affected the structure of EVA. The spectra correspond to the one of the commercial EVA. The molecular vibration is characteristic of functional groups and different type of vibrations. Their wavenumbers are usually found between 400 and 4000 cm^{-1} . For example, the methylene group ($-\text{CH}_2-$) can vibrate in six ways, such as symmetrical stretching, asymmetrical stretching, bending and scissoring and rocking. The spectrum obtained shows some of the previous type of vibrations named:

- 2850, 2918 cm^{-1} : symmetrical and symmetrical stretching of C-H, groups methyl ($-\text{CH}_3$) and methylene ($-\text{CH}_2-$), respectively.
- 1734 cm^{-1} : stretching of the carbonyl group, which belongs to the acetate group.
- 1369, 1464 cm^{-1} : symmetrical and asymmetrical bending from methyl group ($-\text{CH}_3$), together with scissoring of methylene group ($-\text{CH}_2-$). It belongs to the ethylene group.
- 1020, 1235 cm^{-1} : symmetrical and asymmetrical stretching of C-O-C acetates.
- 720 cm^{-1} : Rocking of methylene group ($-\text{CH}_2-$). It belongs to the ethylene group.
- 606 cm^{-1} : Band corresponding to the acetate group. [35]

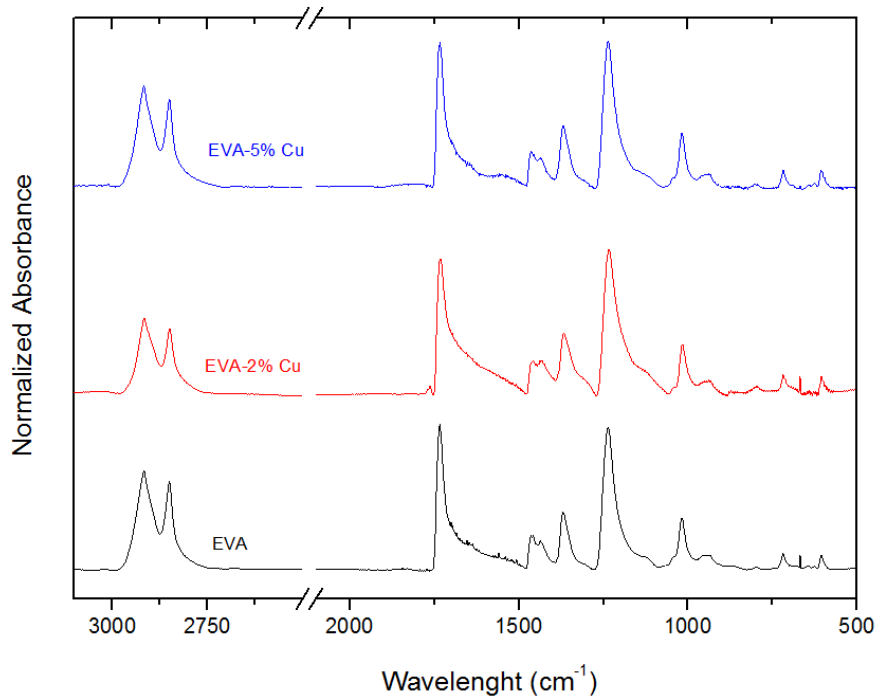


Figure 34. Comparison between the spectra of EVA with different concentrations of Cu nanoparticles. Just to clarify, there is a cut in the spectra between 2270 cm^{-1} and 2390 cm^{-1} , which corresponds to the absorption band of CO_2 .

The conclusion obtained is the inclusion of Cu nanoparticles in different structures does not affect the structure of EVA polymer. Also, comparing the commercial EVA spectrum with the spectrum obtained performing our analysis; it is concluded that the fabrication process doesn't produce changes in the EVA structure. Solution Blow Spinning did not alter the composition from the samples with respect to commercial EVA spectrum (Figure 7).

5.2. DSC results obtained in the analysis and evaluation

Discussion of the DSC analysis will be divided in two parts: heating and cooling.

5.2.1. Heating

In the heating process, the sample undergoes a heating profile from -150 °C till 100 °C at a rate of 10 °C/min. In Figure 35 is observed the endothermic process of heating.

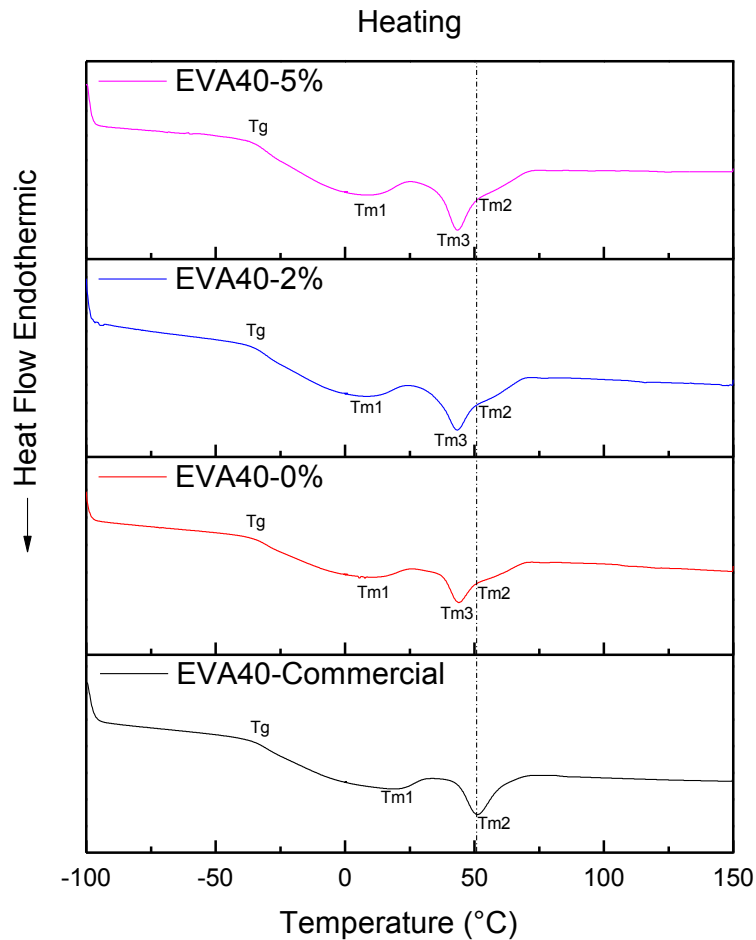


Figure 35. Heating thermogram obtained by DSC.

In Figure 35, the heating thermogram, it can be observed the following characteristics:

1. Glass transition temperature (T_g): it remains the same for the three samples at around -34 °C. The T_g is the temperature or the temperature region in which a polymer stops behaving like a rigid glass and turns to a rubbery state. The T_g appears when the polymer has a percentage of crystallinity or is completely amorphous. In the case of EVA copolymer, the percentage of crystallinity decreases as the percentage in weight of vinyl acetate increases. At 40% in weight of vinyl acetate, crystallinity percentage remains at 4.2% as reported by studies [36]. On the other hand, the glass transition temperature of commercial EVA remains at -20.5 °C, whereas glass transition temperature for amorphous polyethylene is not shown in this plot because is reported to appear at -105°C [37], [38].

2. The range from 0°C till 70°C is assigned to the melting transition of ethylene crystals. It is found because it has a 60% of polyethylene content [39], [40].
3. Main melting temperature (T_{m3}): it is found at 43.7 °C. Other peak, T_{m1} , is observed at 25 °C related with the melting point of a semi-ordered structure of ethylene molecules and a shoulder at 50 °C, those correspond to the melting region. Comparing with commercial EVA, SBS technique lowers the main melting temperature (T_{m3}) of EVA of 51.12 °C, this could be due to internal structural changes in crystallization transitions induced by solvent evaporation [41].

5.2.2. Cooling

In the cooling process, the sample goes following a profile from 100 °C till -150 °C at a rate of 10 °C/min. In Figure 36 is observed the exothermic process of cooling. The thermal history after the heating process is erased.

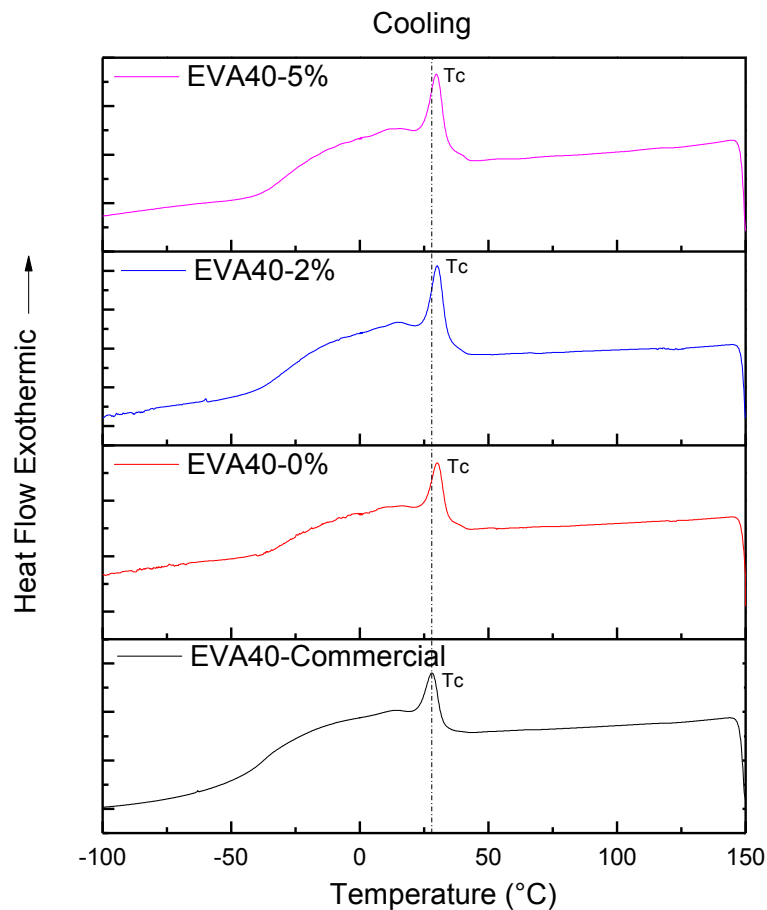


Figure 36. Cooling thermogram obtained by DSC.

In Figure 36, the cooling thermogram, it can be observed the following characteristics:

1. Thermal history was removed after running the heating process.

2. Exothermic peak (T_c): at 30 °C is observed an exothermic peak. It corresponds to the melting temperature peak after losing the thermal story. It has the shape of a partially crystalline polymer. Comparing with commercial EVA, which has a lower value of 28 °C.
3. Glass transition temperature: it is found at around 13 °C. It has a shoulder of -35 °C.

In conclusion, there is no difference in thermal behavior caused by the inclusion of Cu nanoparticles. Both, two processes look consistent and have the same behavior in the same temperatures.

In order to compute the crystallinity grade, X_c , it is used the crystallinity or fusion enthalpy, ΔH seen on Equation 6:

$$X_c = \frac{\Delta H}{\Delta H_m^0} \cdot 100 \quad \text{Equation 6}$$

Where ΔH_m^0 is the enthalpy of fusion of LDPE 100% crystallinity, $\Delta H_m^0 = 277.1 \text{ J g}^{-1}$ [42].

Table 11. Comparison of the results of the DSC analysis obtained.

	T_g (°C)	T_{m3} (°C)	T_c (°C)	ΔH (J/g)	X_c (%)
EVA Commercial	-20.5	51.2	28.06	10.48	3.9
EVA/CU-0%	-34	43.97	30.14	13.48	4.8
EVA/CU-2%	-34	43.37	30.14	14.98	5.4
EVA/CU-5%	-34	43.57	29.74	11.77	4.2

Treating the results obtained from DSC (Table 11), it is concluded that, glass transition temperature doesn't seem to vary as the percentage of Cu nanoparticles increases. It is difficult to determine a concrete value because it is found as a range of temperatures in which the polymer starts behaving as foam. The melting peak (T_{m3}) is clearly observed and does not change much with the increase in weight of Cu nanoparticles. This endothermic peak value is consistent with other studies, which reported about the same melting point which appeared in smaller temperatures, if the percentage of VA content increases. Same happened to the degree of crystallinity, which decreases if the VA content is higher. It is consistent with approximation done in the "Journal of Applied Polymer Science" [36], [42].

SBS process increased the crystallinity degree from commercial EVA, which with the inclusion of Cu nanoparticles seems to lower the crystallinity degree favoring the amorphous nature of the material. The nanoparticles seem to favor the crystallinity degree, increasing it with 2% of Cu nanoparticles. This could be due to the nanoparticles act as nucleation points. Finally, with the increase till 5% of Cu nanoparticles, the crystallinity degree returned to initial values. The fact that there is a greater number of nanoparticles, more agglomerates are formed and the mobility of the chains could increase.

5.3. TGA results obtained in the analysis and evaluation

Results obtained from the Thermogravimetric analysis are presented in two different graphs. The TG curve is the integral form of representation where temperature is plotted versus relative percentage of initial mass. In this graph can be seen the changes in mass of the sample as long as the temperature varies. The second graph obtained is the DTG curve, which is the derivative of the TG curve with respect of time [43].

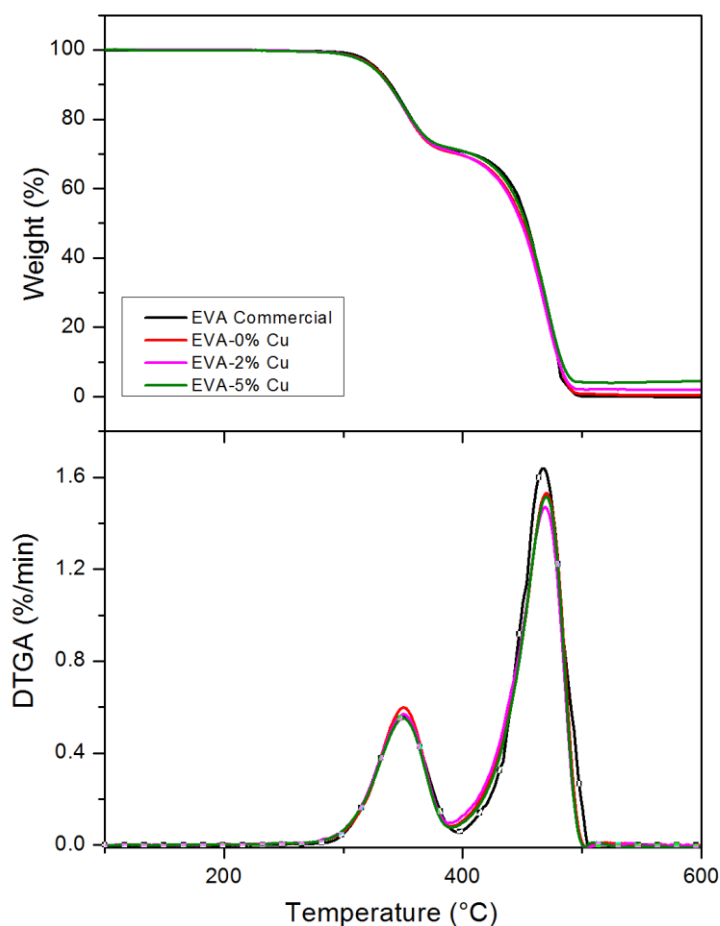


Figure 37. Thermogram for the different concentrations of Cu nanoparticles. It presents the thermal degradation of the samples.

The data plotted correspond to the degradation of EVA nanocomposites and it is a study in terms of mass loss. It is displayed a temperature range from ambient temperature at 25 °C till 600 °C. A few remarkable facts were found:

1. Sudden mass losses: from 300 °C till around 380 °C and from 380 °C till 500 °C. Those sudden losses are clearly seen in the derivative graph (DTGA) and the two peaks observed correspond to maximum degradation regions.
First stage: it is reported as the decomposition of vinyl acetate groups (deacetylation) and there is also the loss of acetic acid, which process ends up forming unsaturated polyenes.
Second stage: it is assigned to random chain scission which generates unsaturated spices, like butane and ethylene [44].

- Comparing to commercial EVA: there is a slightly difference between commercial EVA and EVA nanocomposites created using SBS technique. In first stage, looking at the DTGA plot, it is observed that commercial EVA has grater resistance to thermal degradation when comparing with EVA-Cu 0%. In the second step, SBS improves the thermal degradation from the commercial EVA, furthermore the inclusion of Cu nanoparticles enhanced the resistance to thermal degradation.
- Remnants: when the process reaches the temperature of 500 °C is confirmed that the only leftovers are the Cu nanoparticles percentage in weight. This confirmed that the sample was well prepared and the results are consistent.

Table 12. Percentages of vinyl acetate of the first stage. T1 and T2 are the temperatures of the two peaks of the DTGA, where thermal degradation has its maximum value.

Sample	%VA	%Cu	T ₁ (°C)-VA	T ₂ (°C)-E
Commercial EVA	40.6	0%	350.2	467.2
EVA/Cu-0%	41.5	0%	350.6	470.1
EVA/Cu-2%	40.6	2%	352.1	470.1
EVA/Cu-5%	39.6	5%	350.9	469.9

The percentage of vinyl acetate copolymer can be easily obtained from EVA's thermogram. It was taken into account the decomposition reaction from acetate groups which lead to the formation of acetic acid (Figure 38).

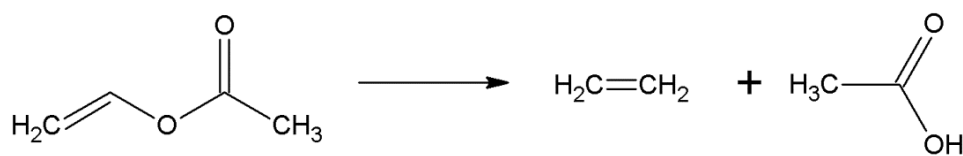


Figure 38. Decomposition reaction from acetate groups.

5.4. SEM results obtained in the analysis and evaluation

Using the scanning electron microscope, SEM, a set of analysis was performed on the samples just after the gold scattering process undergone. It was required to perform this analysis to the different concentrations of Cu nanoparticles, which EVA had, in order to obtain consistent conclusions. Both SE and BSE were used in the scanning process.

Five analyses were done in each of the concentrations of Cu nanoparticles. The specifications are represented in Table 13.

Table 13. Specifications of the different SEM analysis.

Analysis	SE	BSE	Magnification	Voltage
1	✓		250x	10 kV
2	✓		1500x	10 kV
3		✓	1500x	10 kV
4	✓		5000x	15 kV
5		✓	5000x	15 kV

Magnification represents the zooming used. The higher the voltage the better the signal received by the detectors, but a strong voltage can burn and affect the sample.

When images were obtained, using the offline software ImageJ measurements of diameter fibers were done in the sample. It is a technique widely used in scanning microscopy. It consisted in the plot of three vertical lines and the fibers touched were measured by its shortest path (Table 13).

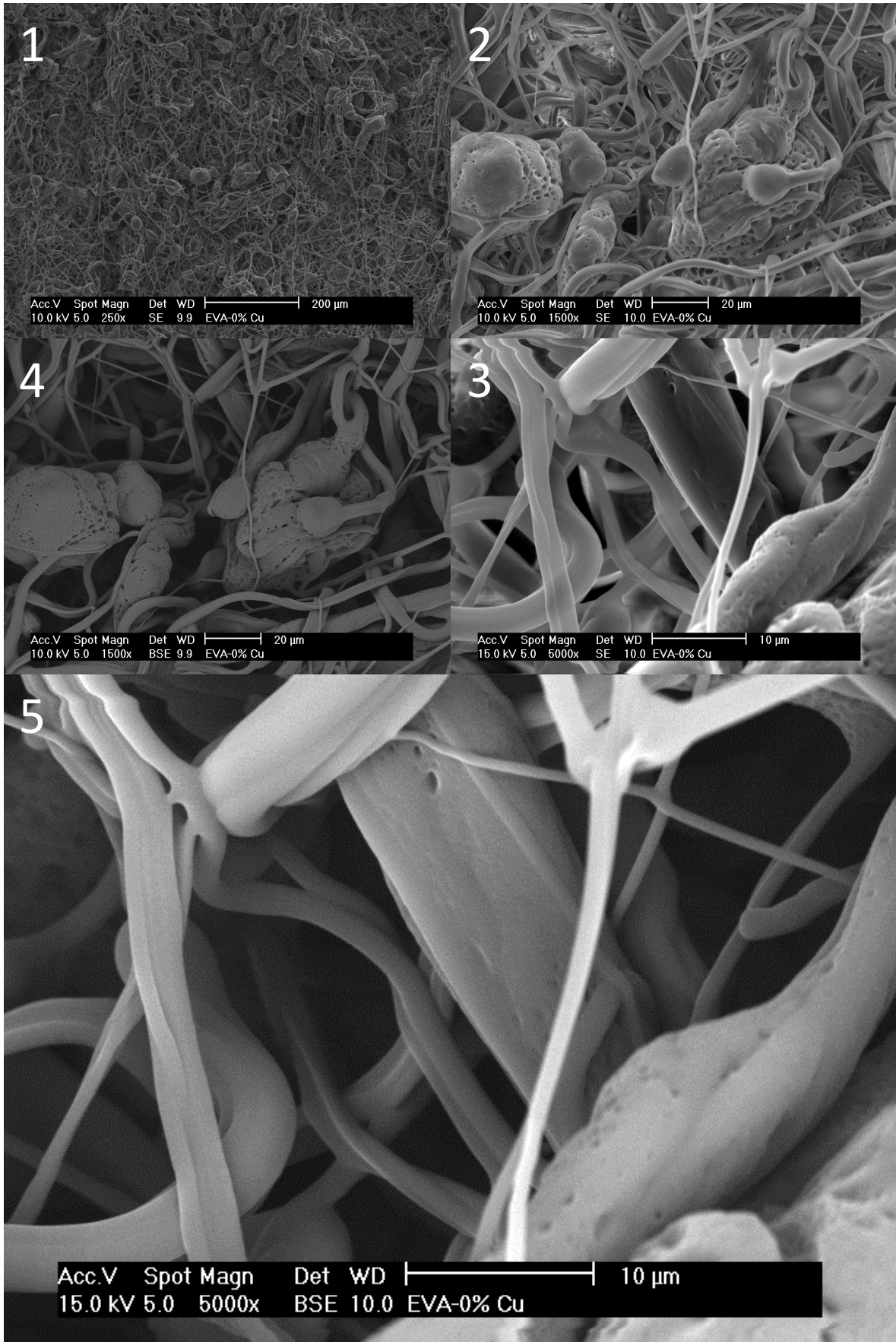


Figure 39. Correspond to EVA/Cu-0%, SEM analysis. 1) 250x SE, 2) 1500x SE, 3) 1500x BSE, 4) 5000x SE, 5) 5000x BSE.

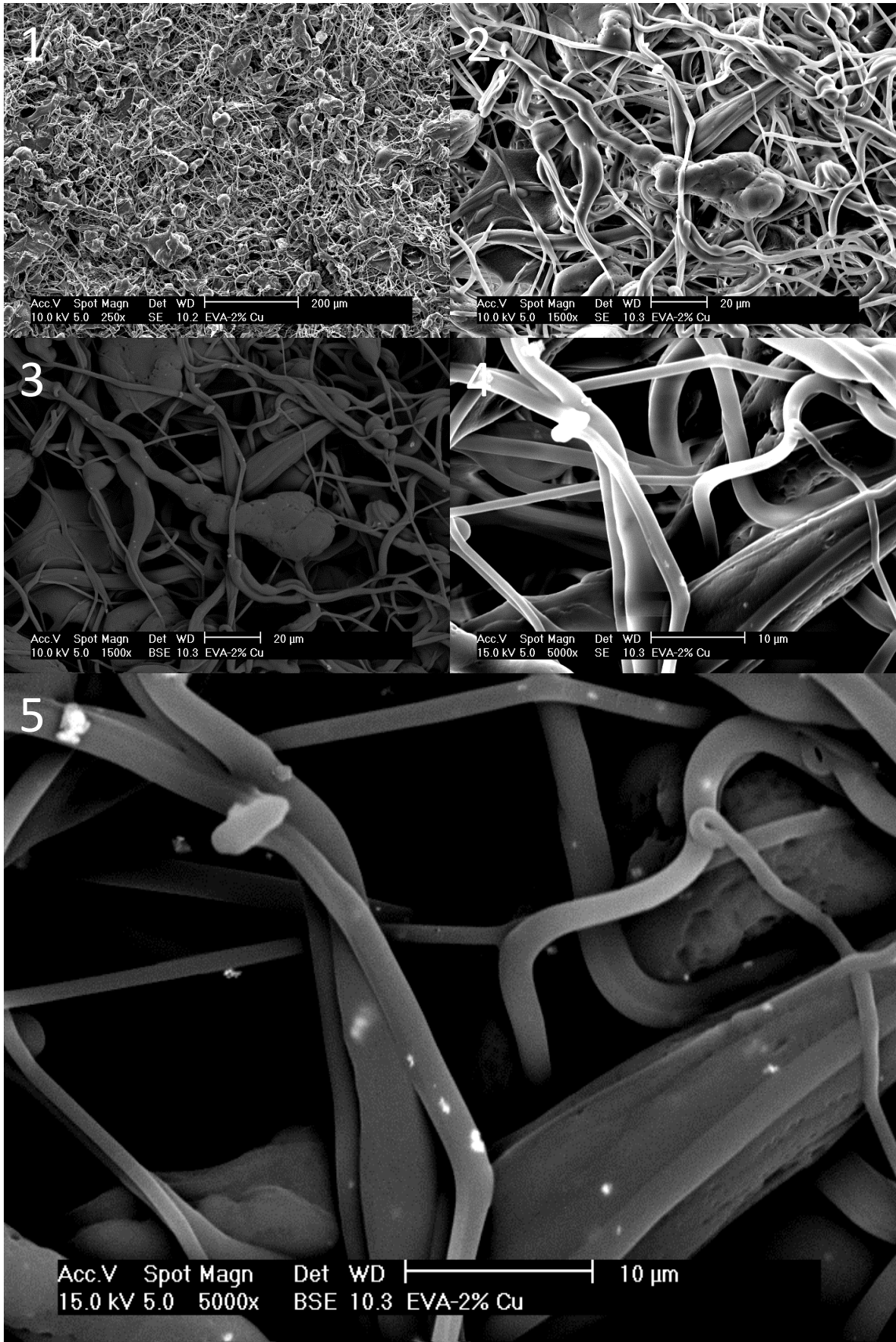


Figure 40. Correspond to EVA/Cu-2%, SEM analysis. 1) 250x SE, 2) 1500x SE, 3) 1500x BSE, 4) x5000 SE, 5) 5000x BSE.

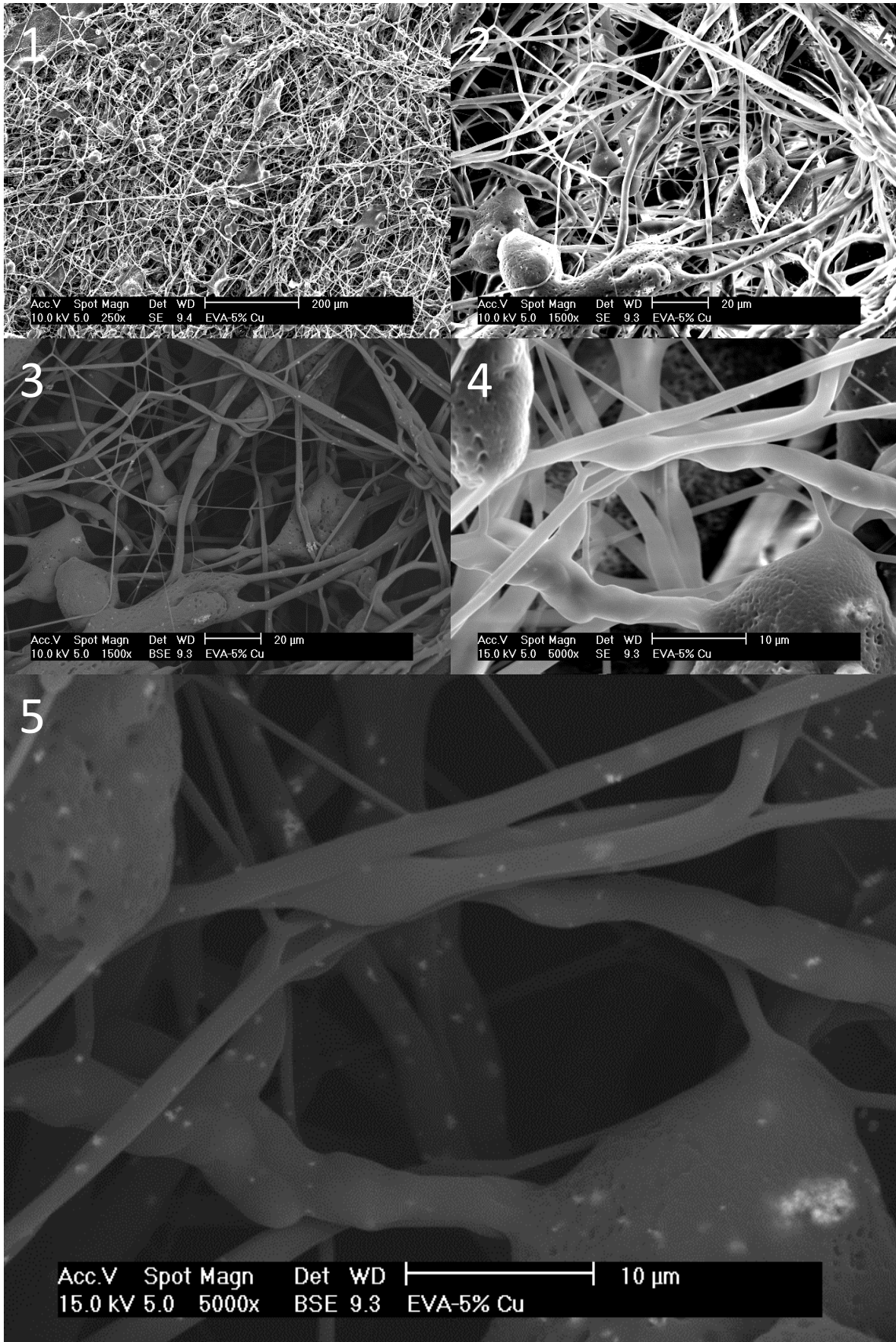


Figure 41. Correspond to EVA/Cu-5%, SEM analysis. 1) 250x SE, 2) 1500x SE, 3) 1500x BSE, 4) 5000x SE, 5) 5000x BSE.

SBS process was able to generate fibers from EVA (40 wt. in Vinyl Acetate) polymer as it is observed. On the first case, EVA/Cu-0% showed that the preparation of the sample was consistent. BSE analysis didn't show impurities or unknown particles in the images. It remarks the good preparation of the samples. SE and BSE analysis shows that the formation of globs is quite evident. This could be caused due to polymer physical properties or a lack of optimization of SBS technique.

Regarding to the second sample, EVA/Cu-2% presented fibers with same morphology as the previous ones. BSE analysis presented the appearance of Cu nanoparticles, which can be observed due to its brighter representation. The dispersion of the particles seems to be as desired, Figure 40(2). Furthermore, Cu nanoparticles are located inside the fibers. Sonification process performed well and dispersed the nanoparticles avoiding cluster formation or other agglomerations.

EVA/Cu-5% had a small fiber diameter on average, which can be seen but is precise measured in Table 14. The dispersion of the fibers was also good and visually more particles can be found in view number 5, when compared to 2% of Cu nanoparticles. Just to notice, in Figure 41(5) on the bottom side of the image, a cluster or agglomeration of Cu nanoparticles is found. The increase in concentration of Cu nanoparticles forms cluster and it is not desired. As a hypothesis, sonification process wasn't as effective as desired and therefore a greater time in time under the ultrasonic bath can solve this situation.

5.4.1. Fiber diameter measurements and analysis

ImageJ, image processing software, was used to measure the fiber diameter and obtain conclusions of how was the performance of SBS process with the established working conditions. For this purpose, three straight lines were plotted in each case and the fibers diameter was measured by its shortest cross-section.

Table 14. Fibers measurements obtained due to the image processing tool.

Sample	Mean	STD	Unit
EVA/Cu-0%	2.52374	1.40808	μm
EVA/Cu-2%	1.62192	0.88917	μm
EVA/Cu-5%	1.1855	0.06619	μm

It is shown the standard deviation, which corresponds to the range of variation and the mean diameter of the fibers for the different concentrations. The measurements were taken at 1500x.

Fiber diameter range was plotted using a histogram (Figure 42), where it can be observed which is the most common fiber's diameter of the different samples created. The results felt similar apart from EVA with 5% of Cu nanoparticles, where it was obtained the smallest diameters. These results show that SBS under the conditions used could vary its results obtained.

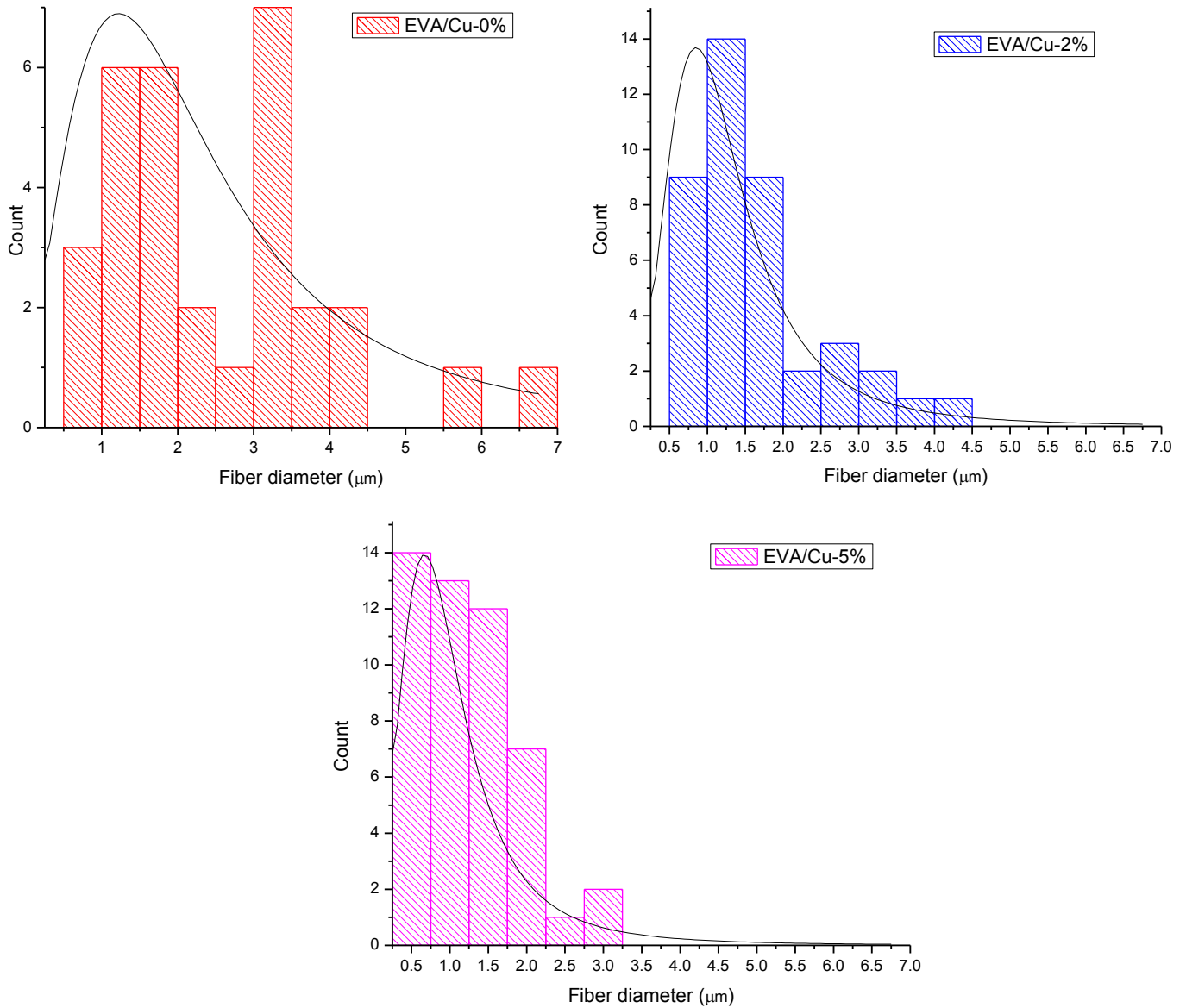


Figure 42. Fiber diameter histogram depending on its concentration of Cu nanoparticles.

5.5. IS results obtained in the analysis and evaluation

The impedance spectroscopy analysis done by the frequency response analyzer. The model used was the 1260 Impedance/Gain-Phase Analyzer by Solartron analytical. Using this powerful system, it was run three analyses per each of the sample concentrations in order to obtain solid conclusions.

The objective was the determination of how does the impedance (Z) varies as a function of the frequency in the three different concentrations. The impedance is a complex variable which can be represented in real and imaginary terms and in polar coordinates, which are modulus and argument (phase). In this case, the second option will provide more valuable information to the project. The prediction is the decrease in the modulus (R) of the impedance as long as the percentage in weight of copper increases.

5.5.1. Impedance modulus (R) analysis

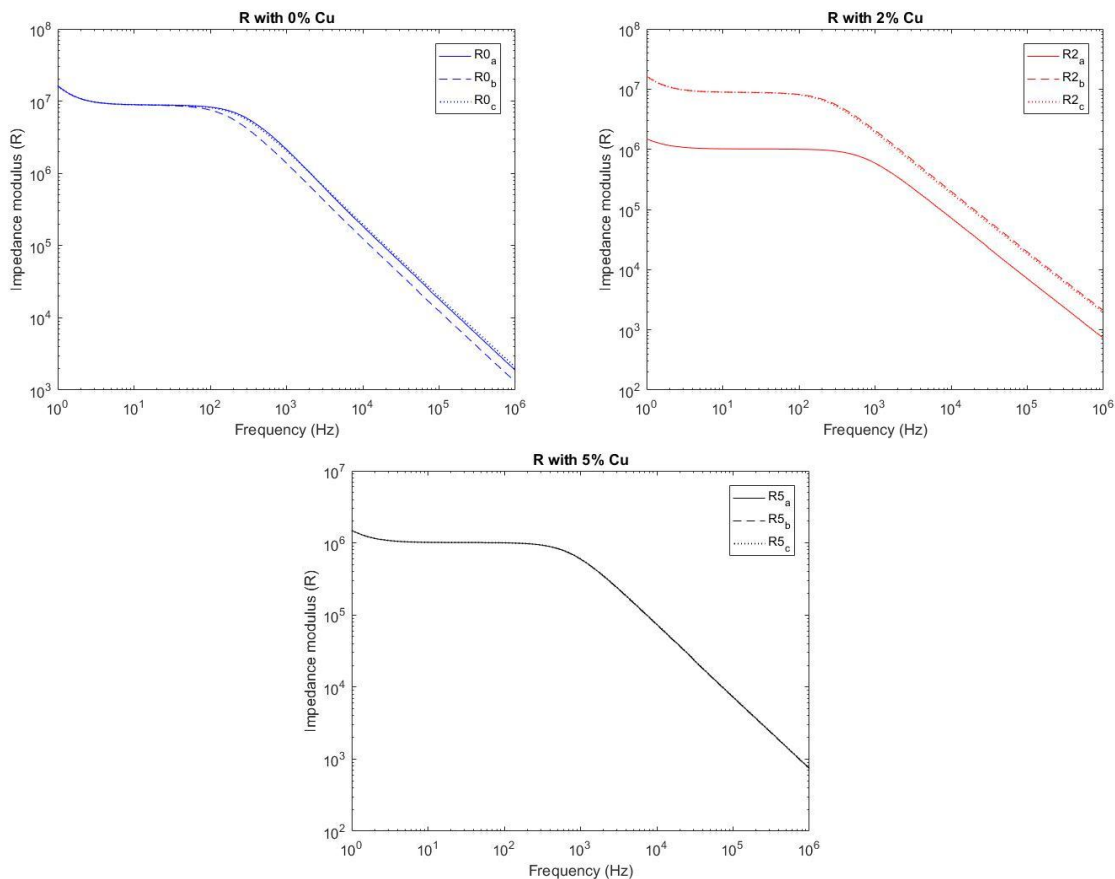


Figure 43. Modulus of the impedance (R), results presented in Ohms.

Different results are obtained in this part. In general, it is observed that the EVA/Cu nanocomposites at low frequency behave like an electrical insulator and in high frequency like a capacitor. The following conclusions were obtained:

- R with 0% of Cu nanoparticles: the results are quite consistent; the three samples plotted have almost the same shape. In the low frequency range (0 – 200 Hz) the resistance modulus remains almost steady at values higher than $10^7 \Omega$. Then when the frequency starts to increase, the resistance starts to decrease linearly. The three samples differ a little with high values of frequency, which can be attributed to the difficulty that SBS should maintain the same thickness uniformly in all the material prepared.

- R with 2% of Cu nanoparticles: in this graph, the results differ. Samples R2_b and R2_c have shapes as the results obtained with EVA with 0% of Cu nanoparticles, whereas sample R2_a has the same shape as the following to be analyzed, EVA with 5% of Cu nanoparticles. This is a curious result and different hypothesis can be obtained:
 - The concentration of 2% of Cu nanoparticles is not enough to obtain consistent results. It reinforces the statement that SBS is a non-uniform process, not only in thickness also in Cu nanoparticles distribution. Samples R2_b and R2_c seem to have not enough concentration of Cu nanoparticles to decrease its impedance, while R2_a does.

 - The concentration of 2% in weight of Cu nanoparticles seems to don't have a consistent behavior. It seems to be small percentage in order to clearly obtain a decrement on impedance modulus.

- R with 5% of Cu nanoparticles: in this graph, there is no doubt that the increment of percentage in weight decreases the impedance of EVA polymer. In the plot, three identically shapes were represented. In the low frequency range, the resistance modulus decreases one order of magnitude till $10^6 \Omega$. It is a great decrement with respect of EVA with 0% of Cu nanoparticles, which had $10^7 \Omega$ at the low frequency range. In the remaining frequency range, it maintains a lower impedance showing more capacitive behavior.

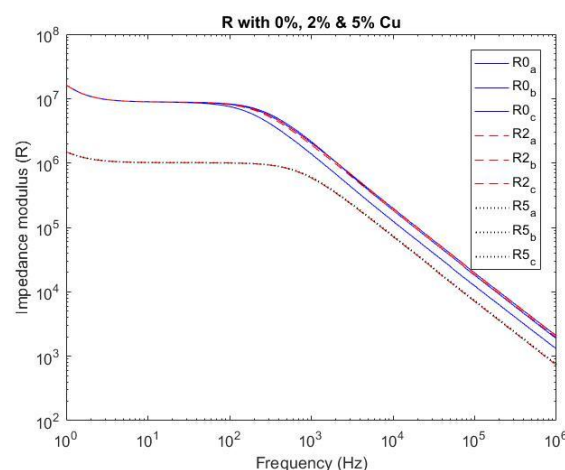


Figure 44. Plot of all the resistance modulus in Ohms (Ω) versus the frequency in Hz, where all the differences previously mentioned are observed.

5.5.2. Impedance phase (ϕ) analysis

Since impedances consist in complex values, the presentation used is in polar coordinates: impedance modulus (R) and impedance phase (ϕ). In this part, the results delivered by the Frequency Response Analyzer were taken to analysis.

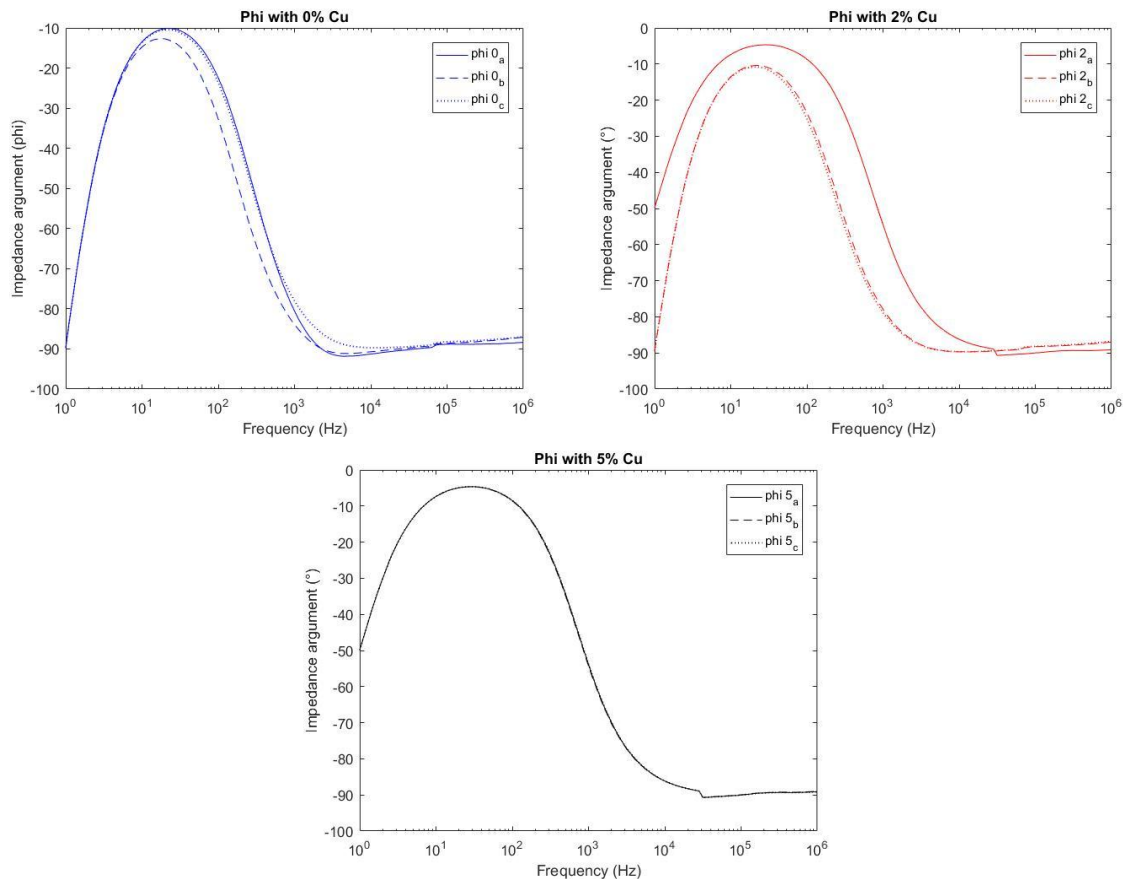


Figure 45. Variation of phase angle (ϕ) with the frequency (Hz)

It is observed in the low frequency range between 0 – 1000 Hz a great variation in phase angle (ϕ) occurs. Focusing on the case of EVA/Cu-0%, near 0 Hz the reactance, X has the greater modulus, moreover all its values are negative, that's why the phase values are negative. At around 1100 Hz the reactance, X lowers its value and the resistance, R increments it, which delivers a lower phase angle reaching -10 degrees. Then, the reactance comes back up and the resistance down, which is maintained till the maximum frequency value (10⁶ Hz).

The inclusion of Cu nanoparticles, as observed in the plot of EVA/Cu-5%, lowers the reactance at low frequencies (near 0 Hz) obtaining lower phase angles and at around 1200 Hz is found its lowest value and lower phase angle, which compared to the previous case there is a significant difference. The phase variation elongates till 10000 Hz compared to the 1100 Hz obtained in EVA/Cu-0%.

In all the three graphs, at high frequency more than 10000 Hz the materials behave as capacitors, whereas at low frequencies varies its behavior between capacitor and insulator.

Table 15. Phase angle electric behavior

Phase angle near - 90 °	Phase angle near 0 °
Capacitor behavior	Insulating (resistor) behavior

To sum up, the inclusion of Cu nanoparticles lowers the reactance, elongates the phase change and as it is going to be seen in the next part enhances the capacitance of the material.

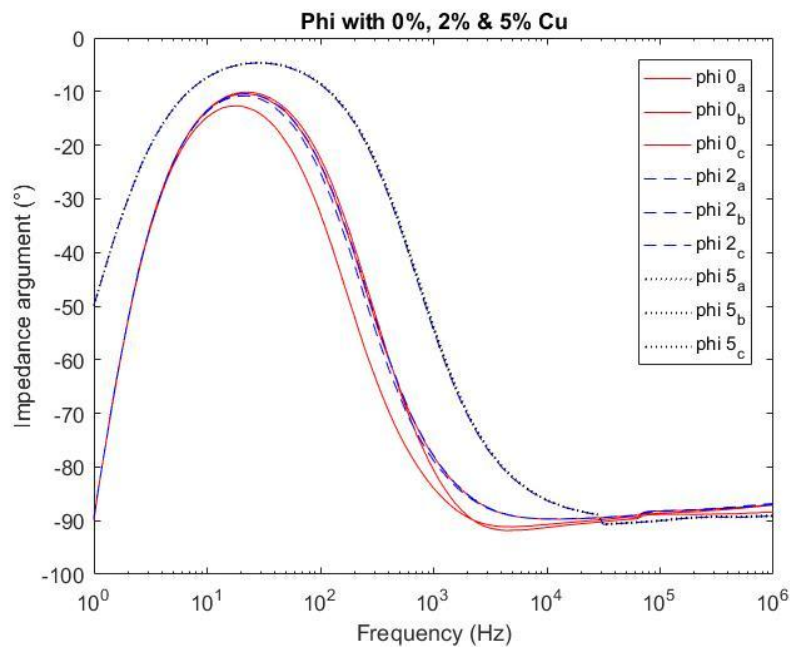


Figure 46. Phase change due to the inclusion of Cu nanoparticles.

5.5.3. Capacitance and dielectric constant analysis

Following with the analysis performed measurements on the capacitance and dielectric constant were taken, experimentally using a digital multimeter and extracted from the data obtained from the impedance spectroscopy analysis.

Using the actual data, that the frequency response analyzer delivered applying the following equation it can be obtained the capacitance of the polymer according to frequency variation: [38]

$$C = -\frac{1}{\omega} * \left[\frac{X}{(R)^2+(X)^2} \right]; \omega = 2\pi f \quad \text{Equation 7}$$

The measured capacitance is then used to compute the dielectric constant, ϵ . It follows the following equation:

$$\epsilon = \frac{Cd}{A} \quad \text{Equation 8}$$

Where d is the thickness of the sample and A , the area of the dielectric.

Capacitance

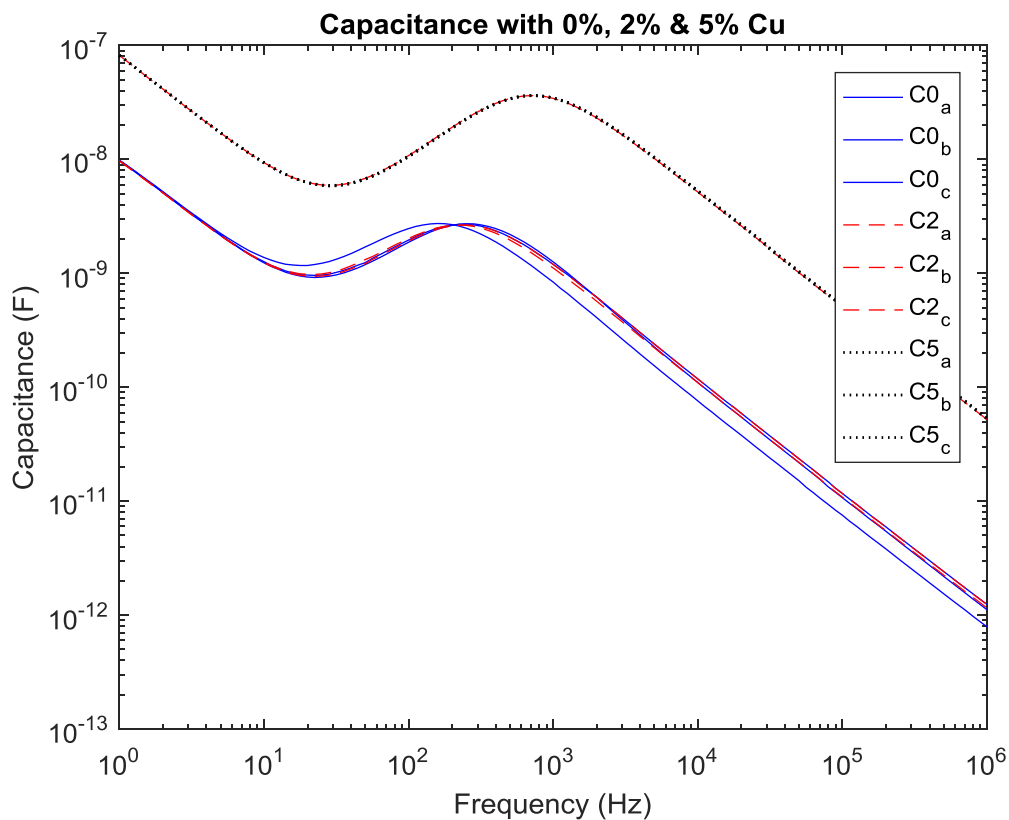


Figure 47. Capacitance variation with the increase in the quantity of Cu nanoparticles.

It is observed an increment of one order of magnitude in capacitance with the inclusion of Cu nanoparticles. This is an expected result the inclusion of these small spherical particles lowers the impedance and increases the capacitance. According to percolation theory, the percolation threshold is not reached. The probability of finding pathways with connect both sides of the dielectric is quite low, spherical nanoparticles had lower volume to mass ratio and thus the material maintains its insulating properties. In this work, just three concentrations of Cu nanoparticles where studied. It is suggested that a greater concentration of Cu nanoparticles would be able to reach the percolation threshold, making this material conductive. It has been reported, that this concentration for LDPE (Low Density Polyethylene) the percolation threshold is found at around 10% of copper. Although, to create a great capacitance material, the concentration of Cu nanoparticles should stay under this threshold [45].

Dielectric constant

The dielectric constant is the ratio between the permittivity of a material and the permittivity of the free space. As the dielectric constant increases, the electric flux density does it to. High dielectric constant materials have greater capacitance and if they have a great high capacity to volume ratio are named supercapacitors. Dielectric constant increases with the inclusion of Cu nanoparticles like the capacitance.

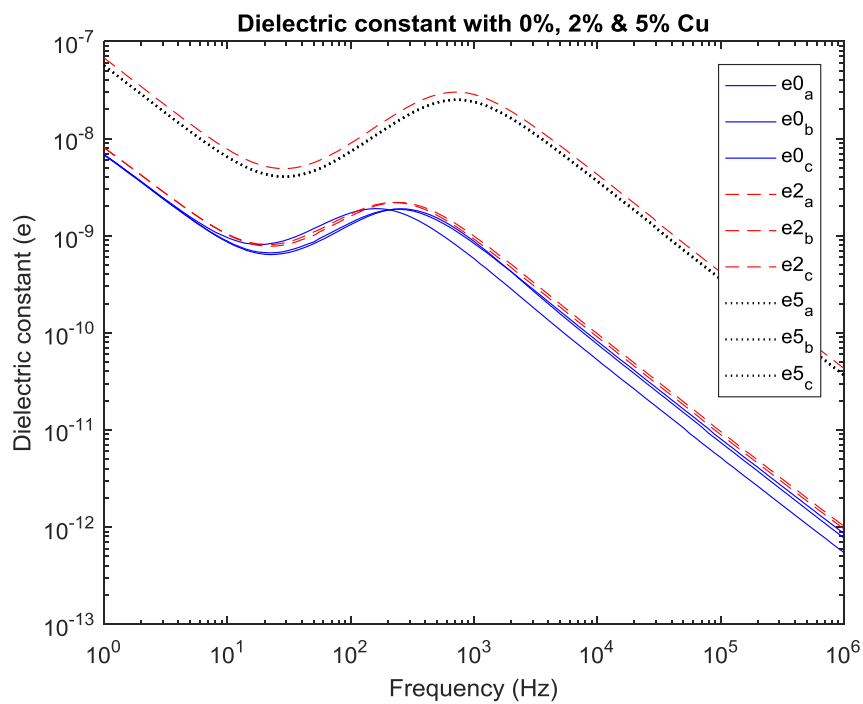


Figure 48. Dielectric constant measurements extracted from the frequency response analyzer.

Table 16. Mean thickness used to evaluate the dielectric constant.

	EVA/Cu-0%	EVA/Cu-2%	EVA/Cu-5%
Mean thickness (μm)	54.5	65	54.2
Standard deviation (μm)	± 6.7	± 4	± 4

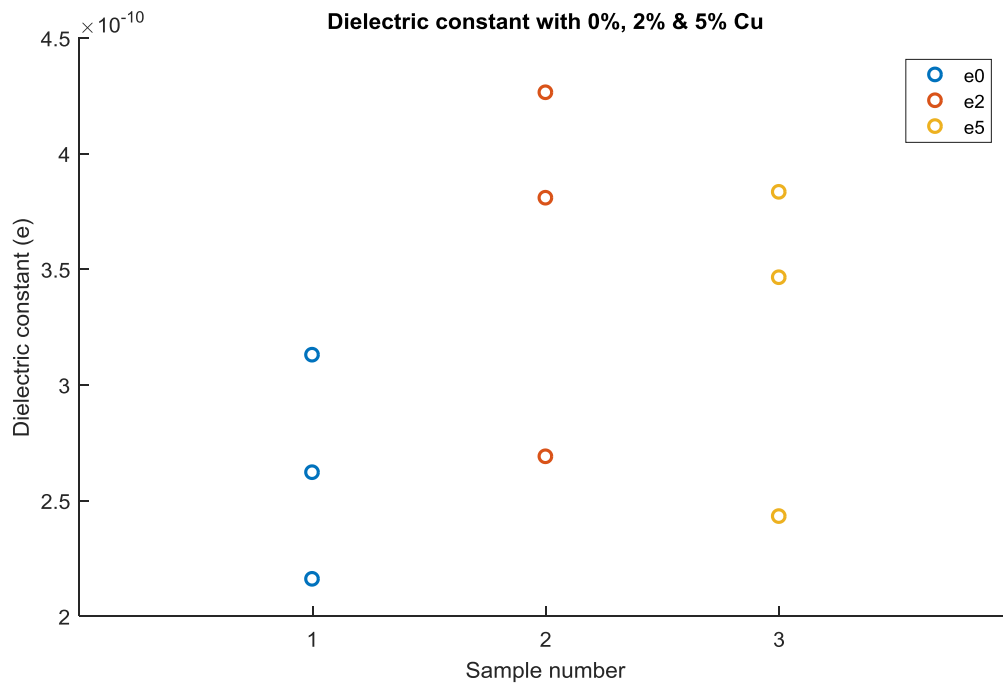


Figure 49. Dielectric constant measurements using a multimeter. Measured at 50 Hz.

Since, it is induced that the concentrations of Cu nanoparticles are under the percolation threshold, in this region the capacitance does not change much and errors can be assumed because the samples are quite thin and can be deteriorated. Experimental results found about the dielectric constant were not conclusive, whereas the ones extracted from the frequency response analyzer showed the same tendency as the capacitance, an increment.

6. Regulatory framework

6.1. Property rights

According to the Law 21/2014, 4 of November 2014, this project is in order with the Intellectual Property Law (IPL) in Spain. The study with educational purposes and scientific research was done under referenced sources and authors. This copy is distributed in the internal network of Universidad Carlos III de Madrid [46].

6.2. Safety measures

National Institute of Workplace Safety and Hygiene (INSHT) presented evaluations about the risk level of nanoparticles, which was inconclusive (NTP 877). Quantifying the exposure was difficult and measure systems inaccurate. Since, the effects are unknown only recommendations can be followed [47].

Therefore, in the laboratory, it is obligatory the use of a laboratory coat in order to prevent harmful fluids to spill in our clothes and protect our skin. Also, to protect the hands it is mandatory the use of standard laboratory gloves. Harmful solvents were used and could enter our organism mostly by inhalation. While they are being utilized, the use of breathing mask and protecting goggles is recommended.

7. Socio-economic environment

7.1. Project's budget

In this section, a budget of the project is presented. It was considered the all the samples prepared, the tools and electricity consumption.

Table 17. Budget of the project.

Budget of the project					
EVA/Cu-0%	Quantity (g)	Price per g	Total	x2 Samples	Total
EVA	1.050 €	0.750 €	0.788 €	1.575 €	3.468 €
Chloroform	6.975 €	0.054 €	0.375 €	0.751 €	
Dichloromethane	6.975 €	0.082 €	0.571 €	1.142 €	
EVA/Cu-2%	Quantity (g)	Price per g	Total	x2 Samples	Total
EVA	1.050 €	0.750 €	0.788 €	1.575 €	3.534 €
Chloroform	6.975 €	0.054 €	0.375 €	0.751 €	
Dichloromethane	6.975 €	0.082 €	0.571 €	1.142 €	
Cu nanoparticles	0.021 €	1.579 €	0.033 €	0.066 €	
EVA/Cu-5%	Quantity (g)	Price per g	Total	x2 Samples	Total
EVA	1.050 €	0.750 €	0.788 €	1.575 €	3.643 €
Chloroform	6.975 €	0.054 €	0.375 €	0.751 €	
Dichloromethane	6.975 €	0.082 €	0.571 €	1.142 €	
Cu nanoparticles	0.055 €	1.579 €	0.087 €	0.175 €	
Total material expenditure	Laboratory material expendable		Electricity consumption	Cost of the project	
10.645 €	4.000 €		4.000 €	18.645 €	

7.2. Future applications and research impact

This work contributes to the research field of nanomaterials, in which new methods used, like Solution Blow Spinning were proved as viable solution to create polymer nanofibers. Using Ethylene-vinyl acetate copolymer was able to generate nanofibers and with the inclusion of Cu nanoparticles the material improved its electrical properties.

This work opens a future path for further research in this field, where materials properties can be improved and this knowledge could be helpful for several applications, like the creation of supercapacitors or the research done by the Department of Material Science of this university about antibacterial properties.

8. Justification of the solution and conclusions

The conclusions for this work can be divided within two groups, the ones extracted from the thermal and morphology analysis and the endpoint reach after the study of the electric behavior.

The allocation of bands was done using FTIR analysis, which delivered consistent spectrum results for the three concentrations of nanoparticles. It was observed no variation in the structure of the polymer and SBS technique did not affect the results. Cu nanoparticles were not captured in the spectrum range analyzed.

According to the results obtained in differential scanning calorimetry, DSC, Ethyl-Vinyl Acetate with Cu nanoparticles filler does not present significant differences in thermal transitions with respect to EVA without filler, but with respect to commercial EVA it has a lower value. Therefore, the addition of nanoparticles does not affect the arrangement of the polymer chains and its chemical behavior. Regarding to the crystallization, the inclusion of Cu nanoparticles affects slightly the degree of crystallinity. Although, comparing SBS processed materials with commercial EVA, it was found a slightly displacement of the glass transition temperature and the melting one to a lower value.

There is not much difference found in TGA thermograms as a function of the content of Cu nanoparticles. It is just found a slightly better resistance to thermal degradation which increases with the concentration of Cu nanoparticles.

Using a frequency response analyzer, the samples were subjected to an impedance spectroscopy. Results presented, determine that the inclusion of Cu nanoparticles lowers the resistance and increases the capacitance of the material. The dielectric constant increased as it did so the capacitance. This solution provided and the fact that the Cu nanoparticles have spherical shape delivered a result in which concentration was not enough to reach the percolation threshold. The capacitance behavior can be improved following those tips approaching near the percolation threshold. This research project helped to provide the beginning of a solution which needs further investigation and it established Solution Blow Spinning technique as a viable and economic solution to create polymeric nanofibers.

9. References

- [1] R. A. Vaia and E. P. Emmanuel, "Polymer Nanocomposites: Status and Opportunities," *MRS Bull.*, vol. 26, no. 5, pp. 394–401, 2001.
- [2] J. Jin, Y. Lin, M. Song, C. Gui, and S. Leesirisan, "Enhancing the electrical conductivity of polymer composites," *Eur. Polym. J.*, vol. 49, no. 5, pp. 1066–1072, 2013.
- [3] G. A. Snook, P. Kao, and A. S. Best, "Conducting-polymer-based supercapacitor devices and electrodes," *J. Power Sources*, vol. 196, no. 1, pp. 1–12, 2011.
- [4] J. F. Cooley, "Apparatus for electrically dispersing fluids. US Patent 692,631," *US Pat. 692,631*, no. 692, pp. 1–6, 1900.
- [5] N. Tucker, J. Stanger, M. Staiger, H. Razzaq, and K. Hofman, "The History of the Science and Technology of Electrospinning from 1600 to 1995.," *J. Eng. Fiber. Fabr.*, vol. 7, no. SPECIAL ISSUE, pp. 63–73, 2012.
- [6] L. H. C. M. Eliton S. Medeiros, Gregory M. Glenn Artur P. Klamczynski, William J. Orts, "Solution Blow Spinning: A New Method to Produce Micro- and Nanofibers from Polymer Solutions," *J. Appl. Polym. Sci.*, vol. 113, pp. 2322–2330, 2009.
- [7] J. P. Jose, S. K. Malhotra, S. Thomas, K. Joseph, K. Goda, and M. S. Sreekala, "Advances in polymer composites: Macro- and microcomposites – state of the art, new challenges, and opportunities," *Polym. Compos.*, vol. 1, pp. 1–16, 2012.
- [8] C. Buzea, I. I. Pacheco, and K. Robbie, "Nanomaterials and nanoparticles: Sources and toxicity," *Biointerphases*, vol. 2, no. 4, p. MR17-MR71, 2007.
- [9] A. Hamrang and B. A. Howell, *Foundations of High Performance - Properties, Performance and applications*. 2014.
- [10] IUPAC, "International Union of Pure and Applied Chemistry Glossary of Basic Terms in Polymer," *Pure Appl. Chem.*, vol. 68, no. 12, pp. 2287–2311, 1996.
- [11] A. M. Henderson, "Ethylene-Vinyl Acetate (EVA) Copolymers: A General Review," *IEEE Electr. Insul. Mag.*, vol. 9, no. 1, pp. 30–38, 1993.
- [12] "Catalyst," *IUPAC Compend. Chem. Terminol.*, vol. 2291, no. Recommendations 1990, p. 2293, 2014.
- [13] N. A. Dhas, C. P. Raj, and A. Gedanken, "Synthesis, Characterization, and Properties of Metallic Copper Nanoparticles," *Chem. Mater.*, vol. 9, no. 1, p. 1446, 2006.
- [14] M. Salavati-Niasari and F. Davar, "Synthesis of copper and copper(I) oxide nanoparticles by thermal decomposition of a new precursor," *Mater. Lett.*, vol. 63, no. 3–4, pp. 441–443, 2009.
- [15] P. K. Khanna, S. Gaikwad, P. V. Adhyapak, N. Singh, and R. Marimuthu, "Synthesis and characterization of copper nanoparticles," *Mater. Lett.*, vol. 61, no. 25, pp. 4711–4714, 2007.
- [16] M. A. J. Uyttendaele and R. L. Shambaugh, "Melt blowing: General equation development and experimental verification," *AIChE J.*, vol. 36, no. 2, pp. 175–186, 1990.
- [17] W. A. G. III, D. W. Brenner, S. E. Lyshchinsk, and G. J. Iafrate, *Handbook of Nanoscience, Engineering, and Technology*. 2003.
- [18] I. Grattan-Guinness, *Landmark Writings in Western Mathematics 1640-1940*. 2005.
- [19] B. Ambravaneswaran, H. J. Subramani, S. D. Phillips, and O. A. Basaran, "Dripping-jetting transitions in a dripping faucet," *Phys. Rev. Lett.*, vol. 93, no. 3, pp. 34501–1, 2004.
- [20] Berndt Wischniewski, "Online - Calculation - Air." [Online]. Available: http://www.peacesoftware.de/einigewerte/luft_e.html. [Accessed: 13-Jun-2017].
- [21] Sigma-Aldrich, "Poly(ethylene-co-vinyl acetate) vinyl acetate 40 wt. %, melt index 57 g/10 min (190°C/2.16kg), contains 200-800 ppm BHT as inhibitor." [Online]. Available: <http://www.sigmaaldrich.com/catalog/product/aldrich/340502?lang=es®ion=ES>. [Accessed: 13-Jun-2017].
- [22] *Hongwu International Group Ltd.* <http://www.hwnanomaterial.com/>. 2016, p. 160721.
- [23] J. S. Taurozzi, V. A. Hackley, and M. R. Wiesner, "Ultrasonic dispersion of nanoparticles for environmental, health and safety assessment – issues and recommendations,"

- Nanotoxicology*, vol. 5, no. 4, pp. 711–729, 2011.
- [24] Fisherbrand, “Fisherbrand 15xxx series, Ultrasonic units.”
- [25] P. R. Griffiths and J. a. de Haseth, *Chapter-2 Theoretical background*. 2007.
- [26] P. Ltd., “Spectrum GX User’s Guide,” *Direct*, 2000.
- [27] C. H. Spink, “Differential Scanning Calorimetry,” *Methods in Cell Biology*, vol. 84. pp. 115–141, 2008.
- [28] METTLER TOLEDO, “DSC822e Differential Scanning Calorimeter (DSC) - Overview.” [Online]. Available: http://www.mt.com/hk/en/home/phased_out_products/PhaseOut_Ana/DSC822e_200_DSC_822e_400.html. [Accessed: 13-Jun-2017].
- [29] METTLER TOLEDO, “Instrucciones de funcionamiento Sistema STAR e de METTLER TOLEDO Módulo DSC822e.”
- [30] M. Suga *et al.*, “Recent progress in scanning electron microscopy for the characterization of fine structural details of nano materials,” *Prog. Solid State Chem.*, vol. 42, no. 1–2, pp. 1–21, 2014.
- [31] G. Höflinger, “Brief Introduction to Coating Technology for Electron Microscopy.” 28-Aug-2013.
- [32] D. H. De Mott, “Frequency Response Analyzer - US3026473A,” 1959.
- [33] H. Allison, “Frequency Response Analyzer - US4322806,” 1982.
- [34] IUPAC, “Beer–Lambert law (or Beer–Lambert–Bouguer law),” in *IUPAC Compendium of Chemical Terminology*, Research Triangle Park, NC: IUPAC.
- [35] A. Marcilla, A. Gómez, and S. Menargues, “TG/FTIR study of the thermal pyrolysis of EVA copolymers,” *J. Anal. Appl. Pyrolysis*, vol. 74, no. 1–2, pp. 224–230, 2005.
- [36] P. M. Kamath and R. W. Wakefield, “Crystallinity of Ethylene-Vinyl Acetate Copolymers,” *J. Appl. Polym. Sci.*, vol. 9, no. 9, pp. 3153–3160, 1965.
- [37] M. Brogly, M. Nardin, and J. Schultz, “Effect of vinylacetate content on crystallinity and second-order transitions in ethylene?vinylacetate copolymers,” *J. Appl. Polym. Sci.*, vol. 64, no. 10, pp. 1903–1912, 1997.
- [38] B. P. Rand, J. Genoe, P. Heremans, and J. Poortmans, “Solar Cells Utilizing Small Molecular Weight Organic Semiconductors,” *Prog. Photovolt Res. Appl.*, vol. 15, no. February 2013, pp. 659–676, 2015.
- [39] M. Borhani Zarandi and H. Amrollahi Bioki, “Thermal and mechanical properties of blends of LDPE and EVA crosslinked by electron beam radiation,” *Eur. Phys. J. Appl. Phys.*, vol. 63, no. 2, p. 21101, 2013.
- [40] K. Agroui, G. Collins, F. Giovanni, and W. Stark, “A Comprehensive Indoor and Outdoor Aging of the Cross-Linked EVA Encapsulant Material for Photovoltaic Conversion,” *Polym. Plast. Technol. Eng.*, vol. 54, no. 7, pp. 719–729, 2015.
- [41] A. Badiie, I. A. Ashcroft, and R. D. Wildman, “The thermo-mechanical degradation of ethylene vinyl acetate used as a solar panel adhesive and encapsulant,” *Int. J. Adhes. Adhes.*, vol. 68, pp. 212–218, 2016.
- [42] S. B. Yamaki, E. a. Prado, and T. D. Z. Atvars, “Phase transitions and relaxation processes in ethylene-vinyl acetate copolymers probed by fluorescence spectroscopy,” *Eur. Polym. J.*, vol. 38, no. 9, pp. 1811–1826, 2002.
- [43] S. E. V Yazovkin, “Thermogravimetric Analysis,” *Charact. Mater.*, pp. 1–12, 2012.
- [44] H. C. Bidsorkhi, H. Adelnia, N. Naderi, N. Moazeni, and Z. Mohamad, “Ethylene vinyl acetate copolymer nanocomposites based on (un)modified sepiolite: Flame retardancy, thermal, and mechanical properties,” *Polym. Compos.*, no. February 2016, 2015.
- [45] M. P. Alvarez, V. H. Poblete, M. E. Pilleux, and V. M. Fuenzalida, “Submicron copper-low-density polyethylene conducting composites: Structural, electrical, and percolation threshold,” *J. Appl. Polym. Sci.*, vol. 99, no. 6, pp. 3005–3008, 2006.
- [46] Gobierno de España, “Ley 21/2014, de 4 de noviembre, por la que se modifica el texto

refundido de la Ley de Propiedad Intelectual,” *Boletín Of. del Estado*, no. 268, pp. 90404–90439, 2014.

- [47] C. Tanarro Gozalo, “NTP 877 - Evaluación del riesgo por exposición a nanopartículas mediante el uso de metodologías simplificadas,” *Inst. Nac. Segur. e Hig. en el Trab.*, pp. 1–6, 2010.